International Immunopharmacology 127 (2024) 111387

Contents lists available at ScienceDirect

International Immunopharmacology

journal homepage: www.elsevier.com/locate/intimp

Nicorandil and carvedilol mitigates motor deficits in experimental autoimmune encephalomyelitis-induced multiple sclerosis: Role of TLR4/TRAF6/MAPK/NF-κB signalling cascade

Aya M. Mustafa [a], Aya M. Shaheen [a], Hala F. Zaki [b], Mostafa A. Rabie [b,*]

[a] Department of Pharmacology and Toxicology, Faculty of Pharmacy, Egyptian Russian University, Cairo, Egypt
[b] Department of Pharmacology and Toxicology, Faculty of Pharmacy, Cairo University, Cairo, Egypt

ARTICLE INFO

Keywords:
Experimental autoimmune encephalomyelitis
Microglia
Nicorandil
Carvedilol
TLR4/MyD88/TRAF6 signalling

ABSTRACT

Multiple sclerosis (MS) is an inflammatory demyelinating neurodegenerative disease that negatively affects neurotransmission. It can be pathologically mimicked by experimental autoimmune encephalomyelitis (EAE) animal model. ATP-sensitive potassium channels (K_{ATP}) plays a crucial role in the control of neuronal damage, however their role in MS are still obscure. Additionally, Carvedilol showed a promising neuroprotective activity against several neurological disorders. Therefore, the present study aimed to investigate the potential neuroprotective effect of K_{ATP} channel opener (nicorandil) as well as α and β adrenoceptor antagonist (Carvedilol) against EAE induced neurodegeneration in mice. Mice was treated with nicorandil (6 mg/kg/day; p.o.) and carvedilol (10 mg/kg/day; p.o.) for 14 days. Nicorandil and carvedilol showed improvement in clinical scoring, behaviour and motor coordination as established by histopathological investigation and immunohistochemical detection of MBP. Furthermore, both treatments downregulated the protein expression of TLR4/ MYD88/TRAF6 signalling cascade with downstream inhibition of (pT183/Y185)-JNK/p38 (pT180/Y182)-MAPK axis leading to reduction of neuroinflammatory status, as witnessed by reduction of NF-κB, TNF-α, IL-1β and IL-6 contents. Moreover, nicorandil and carvedilol attenuated oxidative damage by increasing Nrf2 content and SOD activity together with reduction of MDA content. In addition, an immunomodulating effect *via* inhibiting the gene expression of CD4, TGF-β, and IL-17 as well as TGF-β, IL-17, and IL-23 contents along with anti-apoptotic effect by decreasing Bax protein expression and Caspase-3 content and increasing Bcl-2 protein expression was observed with nicorandil and carvedilol treatments. In conclusion, nicorandil and carvedilol exerted a neuroprotective activity against EAE induced neuronal loss via inhibition of TLR4/MYD88/TRAF6/JNK/p38-MAPK axis besides antioxidant and anti-apoptotic effects.

1. Introduction

Multiple sclerosis (MS) is an inflammatory demyelinating, immune mediated and pathologically complicated disease of the central nervous system (CNS) [1], that is neuropathologically characterized by formation of inflammatory infiltrates, demyelinating plaques, and axonal

Abbreviations: **MS**, Multiple sclerosis; **CNS**, central nervous system; **AD**, Alzheimer's disease; **PD**, Parkinson's disease; **NO**, nitric oxide; **TNF-α**, tumour necrosis factor; **iNOS**, inducible nitric oxide synthase; **ROS**, reactive oxygen specials; **TLRs**, Toll-like receptors; **LPS**, Lipopolysaccharide; **MyD88**, myeloid differentiation factor 88; **TRAF6**, tumour necrosis factor receptor-associated factor 6; **MAPKs**, mitogen-activated protein kinases; **ERK½**, including intracellular signal-regulated kinase ½; **JNK**, c-Jun N terminal; **NF-κB**, nuclear factor-κB; **IL-1β**, interleukin-1β; **BBB**, blood-brain barrier; **EAE**, Experimental autoimmune encephalomyelitis; **KATP**, ATP-dependent potassium; **CCH**, chronic cerebral hypoperfusion; **SCH**, spinal cord homogenates; **CFA**, Complete Freund's adjuvant; **CMC**, carboxy methyl cellulose; **OFT**, Open Field Test; **HB**, hind-base; **FB**, fore-base; **RIPA**, radio immunoprecipitation assay; **BSA**, bovine serum albumin; **AU**, arbitrary unit; **Nrf2**, nuclear factor erythroid-2-related factor-2; **SOD**, super oxide dismutase; **MDA**, malondialdehyde; **H&E**, Haematoxylin and Eosin; **LFB**, Luxol Fast Blue; **MBP**, myelin basic protein; **DAB**, 3, 3′-diaminobenzidine tetrahydrochloride; **HRP**, horseradish peroxidase; **RNS**, reactive nitrogen species; **CD4**, cluster of differentiation 4; **IL-17**, interleukin-17; **TGF-β**, Transforming growth factor-beta; **Th17**, T helper 17; **IRAK-4**, IL-1 receptor-associated kinase-4; **TAK-1**, TGF-β activated kinase-1; **TABs**, TAK1-binding proteins; **K_{ATP}**, ATP-sensitive potassium; **Bcl-2**, B-cell lymphoma 2; **Bax**, Bcl-2 associated X; **caspase-3**, Cysteine-aspartic proteases3.

* Corresponding author at: Department of Pharmacology and Toxicology, Faculty of Pharmacy, Cairo University, Kasr El-Aini Str., 11562 Cairo, Egypt.
E-mail address: Mostafa.mohammed@pharma.cu.edu.eg (M.A. Rabie).

https://doi.org/10.1016/j.intimp.2023.111387
Received 1 November 2023; Received in revised form 27 November 2023; Accepted 12 December 2023
Available online 21 December 2023

damage [2]. Experimental autoimmune encephalomyelitis (EAE), a widely used approach for mimicking MS clinical motor, sensory, and cognitive impairment, is used to examine the pathophysiological mechanisms that contribute to the clinical course of MS and to evaluate potential novel therapeutics for the management of the disease [3].

Microglia-induced neuroinflammation is a significant contributor to the initiation and advancement of neurodegenerative disorders, including as Alzheimer's disease (AD), Parkinson's disease (PD), Huntington's disease, and MS [4–6]. Sustained excessive microglia activation leads to neuronal damage together with neurotoxic substances release, including nitric oxide (NO), tumour necrosis factor (TNF)-α, inducible nitric oxide synthase (iNOS) and reactive oxygen specials (ROS), all of which are implicated in neurodegenerative disorders [7,8]. Toll-like receptors (TLRs), which are essential for the innate immune response, are members of the type I transmembrane receptor family. The majority of these receptors are found on microglia and macrophages [5,9]. Noteworthy, among the TLR family, the activation of TLR4 *via* binding to high-mobility group box 1 protein (HMGB1), a ubiquitous nuclear protein of damage-associated molecular patterns ($DAMP_S$) that released from necrotic cells as a pro-inflammatory cytokine into the extracellular space in response to injury, infection, and inflammation [10]. Indeed, TLR4 activation results in recruitment of myeloid differentiation factor 88 (MyD88) to stimulate tumour necrosis factor receptor-associated factor (TRAF)-6 to activate mitogen-activated protein kinases (MAPKs) family that finally led to nuclear factor-kappa B (NF-κB) activation. The latter trigger the transcription of a range of pro-inflammatory factors, such as interleukin-1β (IL-1β), TNF-α, IL-6, and iNOS [11,12]. Additionally, the proliferation of CD4+ T cells, which are crucial for the development of experimental autoimmune encephalomyelitis (EAE), is augmented by TLR4 activation [13]. Autoimmune disorders are thought to develop and advance via the TLR-MyD88 signalling pathway [14] in addition to its role in the pathogenesis of EAE induced MS *via* controlling dendritic cell antigen presentation, disruption the integrity of the blood–brain barrier, and T and B cells activation [15].

Indeed, ATP-dependent potassium (K_{ATP}) channel controls cellular metabolism together with electric activity [16] that is expressed mainly in microglia [17,18]. It was reported previously that K_{ATP} channel is implicated in brain ischemic injury, and K_{ATP} channel knockdown exacerbates ischemic injury via amplifying reactive glia and inflammatory responses [19]. In addition, other studies revealed that K_{ATP} channels play crucial role in regulating inflammatory responses that is involved in disease pathogenesis [20,21]. Noteworthy, nicorandil, a K_{ATP} channel opener, attenuated chronic cerebral hypoperfusion (CCH) induced impaired learning and memory *via* decreasing serum nitrosative stress, brain oxidative stress and inflammation [22]. Moreover, nicorandil has been reported to exert a neuroprotective effect against HD [23] and PD [24]. Furthermore, nicorandil attenuates inflammasome activation and TLR4 signalling cascade to guard against inflammation generated by oxygen-glucose deprivation in BV-2 cells [25].

In parallel, carvedilol, is an antihypertensive drug with non-selective β-adrenergic and selective α-adrenergic blocking activities that have been used clinically in congestive heart failure and left ventricular dysfunction [26]. Carvedilol is reported to possess anti-inflammatory effect *via* downregulating TLR4 expression and inhibiting its downstream signalling transduction [27]. Moreover, carvedilol demonstrated a neuroprotective effect against several models of transient focal stroke through free radical scavenging properties [28]. According to the aforementioned data, the current study was designed to investigate the neuroprotective effect of K_{ATP} channel opener, nicorandil, and carvedilol against EAE-induced MS with emphasis on TLR4/ p38MAPK/NF-κB signalling transduction.

2. Materials and methods

2.1. Ethics statement

The research adheres to the ARRIVE guidelines and the National Institutes of Health's Guide for the Care and Use of Laboratory Animals (NIH publication No. 85–23, revised 2011), both of which were endorsed by the Ethics Research Committee of the Faculty of Pharmacy, Cairo University (Cairo, Egypt; Permit number 3195). Every possible effort was made to reduce animal suffering throughout the experiment.

2.2. Animals

Male Swiss albino mice, weighing 18–25 g, were used. Additionally, for EAE induction, the spinal cord from male Sprague–Dawley rats weighing 200–250 g was mixed with the same volume of complete Freund's adjuvant (CFA). All animals were obtained from the animal facility of Faculty of Pharmacy, Cairo University (Cairo, Egypt). Animals were allowed to acclimate to laboratory conditions for one week before starting the experiment. One week was allotted for the animals to acclimate to laboratory conditions prior to the commencement of the experiment. The animals were maintained in controlled environments with a light–dark cycle of 12 h, humidity at 60 ± 10 %, and a constant temperature of 23 ± 2 °C. Ad libitum water and standard chow diet were unlimitedly provided to the mice, and all behavioural examinations were conducted in a laboratory with adequate insulation.

2.3. Induction of experimental autoimmune encephalomyelitis (EAE) and clinical scoring

EAE was actively induced using the Sprague–Dawley rat spinal cord (SCH) (1 g spinal cord mixed with the same volume of complete Freund's adjuvant (CFA) (Sigma-Aldrich, MO, USA) and thoroughly emulsified using a sonicator. Each mouse was immunized with a subcutaneous injection (100 μl) on day 0 and 7 at two separate sites on the back [29]. EAE clinical score was determined daily by a blinded observer based on the degree of paralysis on a scale from 0 to 7: no symptoms (normal) = 0; partial tail paralysis = 1; full tail paralysis = 2; hindlimb weakness = 3; partial hindlimb paralysis = 4; full hindlimb paralysis = 5; partial forelimb paralysis = 6; moribund state or death = 7 [30].

2.4. Experimental design

Mice were randomly divided into six groups, (n = 12/group); Group I received normal saline containing 0.5 % w/v carboxy methyl cellulose (CMC) (0.2 mL; p.o.; Sigma-Aldrich, MO, USA) and served as normal control group. Group II received nicorandil (6 mg/kg/day; p.o.; Sigma-Aldrich, MO, USA) [31]. Group III received carvedilol (10 mg/kg/day; p.o.; Sigma-Aldrich, MO, USA) [32]. Groups IV-VI were immunized with SCH in CFA at days 0 and 7 (100 μl; s.c.), whereas group IV was left untreated, meanwhile group V received nicorandil (6 mg/kg/day; p.o.) [31] and group VI. received carvedilol (10 mg/kg/day; p.o.) [32]. All treatments were conducted for 14 days, whereas nicorandil and carvedilol were suspended in saline containing 0.5 % w/v CMC. The animals underwent behavioural evaluations on day 15 and 16, after which they were euthanized and their entire brains were rapidly removed, rinsed with ice-cold saline, flash-frozen in liquid nitrogen, and subsequently kept at −80 °C. Isolated brains were subsequently categorized randomly into three subsets. The first subset (n = 3/group) was employed to evaluate parameters using western blot technique after immersing with RIPA buffer provided with protease and phosphatase inhibitors. Meanwhile, in the second subset (n = 6/group), the brain was divided into 2 hemispheres; the right one (n = 6) was homogenised with phosphate buffer saline (PBS) to measure parameters by ELISA and the left one (n = 6) was submerged with lysis buffer to evaluate parameters via PCR

method. Finally, the last subset (n = 3/group) were fixed in 10 % formol saline for histopathological analysis of the corpus callosum and immunohistochemical evaluation of myelin basic protein (MBP). Scheme 1 provides a comprehensive overview of the chronological sequence of behavioural assessments and interventions.

2.5. Behavioural tests

Behavioural investigations were conducted throughout the light cycle starting from 8am for two consecutive days. On the initial day, the open field and rotarod tests were performed, followed by the grid walk assignment and footprint tests on the subsequent day, with a two-hour interval between each test [6]. The open field test involved the utilization of ANY-Maze video tracking software (Stoelting Co, USA) to monitor the movement patterns of animals.

2.5.1. Open field test (OFT)

The objective of the open field test was to estimate spontaneous locomotion. The experimental setup comprised a cubic box constructed of wood, measuring 44 × 44 × 44 cm. The floor was polished black and the walls were red. White lines partitioned the box into sixteen equal squares. For five minutes after being individually positioned in the apparatus's center, the mice were permitted to investigate the field. The animals were observed, and data collected using an overhead camera. Various metrics were recorded, including the total distance travelled, mean speed, time immobile, and the number of rearing frequencies, which refers to the count of rearings performed on the hind limbs, using an overhead camera and the data were analysed using ANY-Maze video tracking software (Stoelting Co, USA). To prevent interference, the floor was cleansed following each animal examination [33].

2.5.2. Rotarod test

The rotarod apparatus was utilized to assess motor coordination and grip strength. The apparatus measured 120 cm in length, with a diameter of 3 cm, was partitioned into five compartments using discs with a diameter of 24 cm, and were subjected to a constant rotational speed of 25 rpm. Animals underwent training sessions for three days prior to experimental procedures. Those that maintained their position on the rod for a duration of five minutes were selected to participate in the experiment. The test was executed following the performing of OFT, and the time for mice to fall was documented manually as fall-off latency [29].

2.5.3. Grid walk task test

A metal square grid with raised properties, measuring 32 cm × 20 cm × 50 cm, was utilized. Each grid cell inside the structure had an entrance with a diameter of 11 x 11 mm. The grid equipment was situated within a chamber designed to reduce sound transmission, and the space was illuminated with low-intensity illumination. Following each experiment, the device was cleaned using a solution consisting of 70 % ethanol. The camera was positioned beneath the equipment at an approximate angle ranging from 20 to 40 degrees in order to evaluate the animals' foot-faults, namely their stepping errors. The animals were allotted a duration of 5 min to traverse the elevated wire surface. The actions exhibited on the grid were documented and subsequently subjected to analysis. The number of foot-faults for each limb was tallied manually and subsequently compared to the total number of steps taken by that particular limb. A step was deemed to be a foot-fault when it failed to provide support and the foot passed through the aperture of the grid [34].

2.5.4. Footprint test

Black nontoxic paint was applied to the forefeet and the hindfeet of mice in order to obtain footprints. After providing the animals with access to a confined rectangular box contains runway that possesses the following dimensions: a length of 50 cm, a width of 10 cm and walls that are 10 cm in height, a sheet of white paper was positioned on the runway's floor. We determined the walking pattern of each mouse manually by calculating the mean distance travelled of one foot using 3 hind paw strides when the animal moves at constant rate as stride length and the average side-to-side distance between the two hind paws as stride width [33].

2.6. Biochemical parameters

2.6.1. Western blot analysis of TLR4, MyD88, TRAF6, (pT183/Y185)-JNK, p38 (pT180/Y182)-MAPK, Bax and Bcl-2

To maintain protein integrity, the first subset of brains was subjected to homogenization using RIPA lysis buffer (50 mM Tris HCl, 150 mM NaCl, 0.1 % SDS, 0.5 % sodium deoxycholate, and 1 % Triton X-100 at pH 8) and a cocktail of freshly prepared protease-phosphatase inhibitors. Assay Kit for Bradford Protein (Bio BASIC INC, ON, Canada):

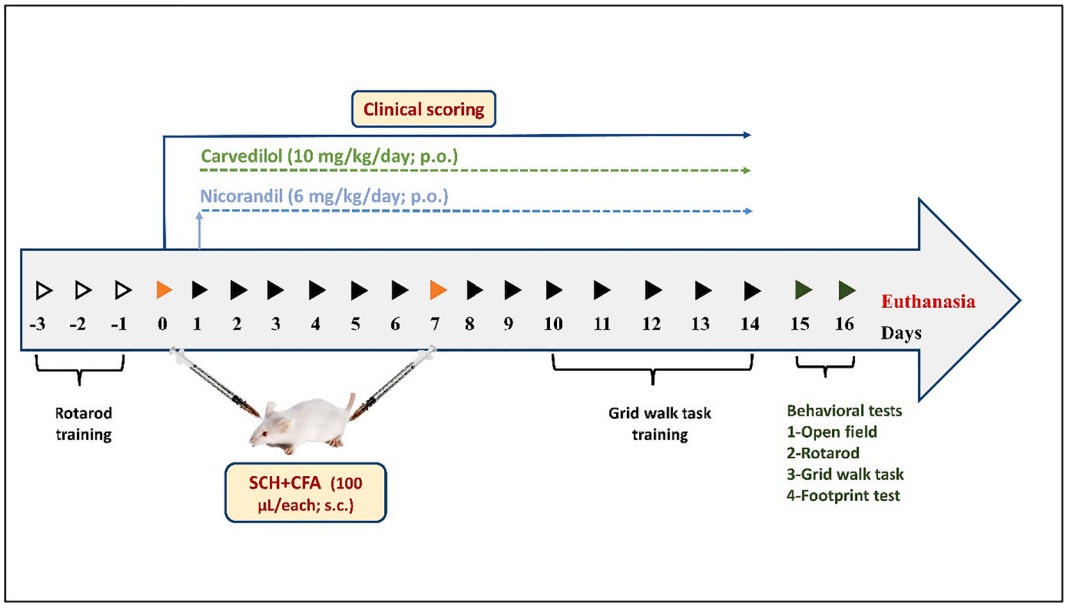

Scheme 1. Chronological sequence for experimental design and behaviourial assessment.

This kit was utilized to quantify proteins. A 5 min boiling of 10 μg protein concentration from each sample in Laemmli buffer was followed by separation by SDS-PAGE and transfer to a PVDF membrane that had been immobilized with 5 % bovine serum albumin (BSA). In order to assess protein expression, a membrane was incubated with primary antibodies (Thermo Fisher Scientific, MA, USA) against TLR4 (2 μg/ml; cat#: PA5-23124), MyD88 (1:1000; cat#: 14-6223-63), TRAF6 (1:1000; cat#: PA5-29622), (pT183/Y185)-JNK (1:1000; cat#: 44-682G), p38 (pT180/Y182)-MAPK (1:1000; cat#: 44-684G), Bax (1:2000; cat#: PA5-11378), Bcl-2 (1:1000; cat#: PA5-27094) and β-actin (1:1000; cat#: PA1-183) polyclonal antibody on a roller shaker at 4 °C overnight For two hours, at room temperature, secondary antibodies were subsequently used to probe the membranes (Dianova, Hamburg, Germany). Densitometric analysis was employed to determine the quantity of target proteins using image analysis software integrated into the ChemiDoc™ MP Imaging System (version 3) (Bio-Rad, CA, USA). Ten percent acrylamide was utilized for each protein under investigation. After normalizing for β-actin protein expression, the results were presented in arbitrary units (AU).

2.6.2. ELISA assay of NF-κB p65, IL-6, IL-1β, IL-23, IL-17, TGF-β, TNF-α and Nrf2

In the second subset, brains (right hemispheres) were homogenized in phosphate buffer saline (PBS), where MyBioSource ELISA kits (CA, USA) were utilised to ascertain NF-κB p65 (cat#: MBS2505513), IL-1β (cat#: MBS825017), interleukin-23 (IL-23) (cat#: MBS2023294), Nrf2 (cat#: MBS752046), TGF-β (cat#: MBS175818) and IL-17 (cat#: MBS2508197). In addition, TNF-α was quantified using kits purchased from Cusabio (Wuhan, PRC; cat#: CSB E11987r) and IL-6 was assessed using Elabscience ELISA kit (Wuhan, PRC; cat#: E-MSEL-M0001). The manufacturer's prescripts were followed, and the outcomes were displayed as pg/mg protein for NF-κB p65, IL-6, IL-1β, IL-23, TNF-α, TGF-β and IL-17, ng/mg protein for Nrf2. In parallel, Colorimetric assay kits (Biodiagnostic, Cairo, Egypt) were used to assess superoxide dismutase (SOD) activity and lipid peroxidation biomarker measured as malondialdehyde (MDA) in adherence to the guidelines provided by the manufacturer. The results were presented as U/gm protein for SOD and as nmol/gm protein for MDA.

2.6.3. Quantitative RT-PCR

In lysate buffer, brains were homogenized in order to assess the mRNA expression of Caspase-3, CD4, TGF-β, and IL-17. Brain tissue was processed for total RNA extraction using the RN easy Mini kit (Qiagen, Venlo, Netherlands). The purity of the extracted RNA was determined spectrophotometrically at 260/280 nm. cDNA was transcribed from equal quantities of RNA (1 μg) using the Reverse Transcription System (Promega, Leiden, Netherlands) in accordance with the protocol provided by the manufacturer. Using SYBR Green Master Mix (Applied Biosystems, CA, USA), quantitative RT-PCR was executed on CD4, TGF-β, IL-17, and Caspase-3. In summary, a 25 μl reaction mixture was prepared by combining 5 μl of cDNA with 12.5 μl of SYBR Green mixture, 5.5 μl of RNase free water, and 2 μl of each primer. The primer sequences are detailed in Table 1. Forty cycles were utilized to complete the PCR amplifications: 15 s at 95 °C for denaturation, 60 s at 60 °C for annealing, and 60 s at 72 °C for extension. In order to calculate the relative expression of target genes, the $2^{-\Delta\Delta CT}$ formula was employed, where the expression levels were first normalized to β-actin [35].

Table 1
Primer sequences used for qPCR.

mRNA species	Accession number	Primer sequence (5′–3′)
CD4	NM_001001908.2	F: GTAAGAGAAGCAGAGGGGAAGAG R: GATTCTTGATGATCAGGGGAAAG
TGF-β	NM_011577.1	F: TGCTAATGGTGGACCGCAA R: CACTGCTTCCCGAATGTCTGA
IL-17	NM_002190.3	F: CGGACTGTGATGGTCAACCTGA R: GCACTTTGCCTCCCAGATCACA
Caspase-3	NM_012922.2	F: GTGGAACTGACGATGATATGGC R: CGCAAAGTGACTGGATGAACC
β-actin	NM_007393.5	F: GAGACCTTCAACACCCCAGC R: ATGTCACGCACGATTTCCC

2.7. Histopathological examination

Brain tissue specimens (n = 3/group) were subjected to fixation using 10 % neutral buffered formalin for a duration of 72 h, after which the formalin solution was changed on a daily basis. Following trimming and processing in successive grades of ethanol, xylene was used to clear the samples, followed by the process of infiltrating, and embedding synthetic wax into paraplast tissue embedding media. Sagittal brain sections with a thickness of 5 μm were sectioned using a rotatory microtome. Haematoxylin and Eosin (H&E) as well as luxol fast blue (LFB) stains were performed for investigation of corpus callosum in brain samples as lesions in this area are important clue in the diagnosis of multiple sclerosis [29]. Tissues stained with H&E were examined under light microscope for assessment of corpus callosum [36]. Moreover, LFB staining was employed to determine the average proportion of myelinated nerve fibers in the corpus callosum using six non-overlapping fields for analysis. Indeed, Leica application module-operated full HD microscopic camera (Leica Microsystems GmbH, Wetzlar, Germany) was utilized to acquire all micrographs and data for histological analysis [37].

2.8. Immunohistochemical detection of MBP

Deparaffinised 5 μm thick brain tissue section were cut and prepared for evaluation of Mylin basic protein (MBP). Tissue sections underwent treatment with a 3 % hydrogen peroxide solution for a duration of 20 min. Following this, they were rinsed with PBS and subsequently subjected to an overnight incubation at a temperature of 4 °C with an Anti-MBP antibody (Abcam, ab209328, 1:100). After subjecting sections to a PBS wash, they were incubated with secondary antibody (Dako, Carpenteria, CA, USA) for a duration of 20 min then with horseradish peroxidase HRP Envision reagent (Dako, Carpenteria, CA, USA) for a duration of 20 min. After another wash with PBS, the reaction was observed for 10 min using 3, 3′-diaminobenzidine tetrahydrochloride (DAB Substrate Kit, Vector Laboratories Inc., Burlingame, CA, USA). In preparation for microscopic examination, sections were subsequently dehydrated, clarified in xylene, counterstained with haematoxylin. The average percentage area of MBP immunohistochemical expression in immunostained tissue sections was calculated, without including non-specific DAB staining or DAB depress (if found) or negative blue background, by analysing six arbitrarily non-overlapping fields from the corpus callosum region using Leica application module-operated full HD microscopic camera (Leica Microsystems GmbH, Wetzlar, Germany) [29]. Indeed, positive control was stained with the whole process including primary antibody incubation process, whereas in negative control, staining process was carried out without the primary antibody used in the incubation step.

2.9. Statistical analysis

All data determined were expressed as mean ± S.D. Results were analysed using one-way analysis of variance test (one-way ANOVA) followed by Tukey's multiple comparison test for all parameters. The clinical scoring was analysed utilizing two-way ANOVA and the Bonferroni multiple comparisons post hoc test. The statistical analysis was conducted utilizing version 5 of the GraphPad Prism software. In all statistical analyses, a significance $p < 0.05$ was established.

3. Results

No statistically significant differences were observed among the control group (Gp1), nicorandil group (Gp2), and carvedilol group (Gp3) for all measured parameters. Therefore, all subsequent comparisons were made relative to the control group.

3.1. Effect of nicorandil and carvedilol on clinical scoring in EAE mice

As depicted in Fig. 1, Mice injected with spinal cord homogenate and CFA demonstrated an increment in EAE clinical signs that was worsening by time indicating disease progression. The severity of EAE clinical sign increased after the second immunization and was witnessed by paralysis of both hind- and forelimbs at the end of the study (median = 5.2), as compared to control group. Alternatively, mice treated with nicorandil, and carvedilol showed an improvement in EAE clinical signs, as compared to the insult and almost all animals appears as control group.

3.2. Effect of nicorandil and carvedilol on behaviour and motor incoordination in EAE mice

Multiple sclerosis (MS) causes brain damage and neuronal loss with subsequent motor incoordination. In Figs. 2 and 3, EAE mice displayed marked reduction in distance travelled (93 %), mean speed (89 %), and rearing frequency (93 %) in open field test (OFT) as well as fall-off latency (96 %) in rotarod test, along with increase in time immobile by 3.2-folds in OFT, when comparing to control group. In parallel, the insult group demonstrated an upsurge in %foot fault by 8.7-folds in grid walk test together with an obvious decline in both stride length and width by 46- and 36 %, respectively in footprint test, relative to control group.

In opposition, nicorandil and carvedilol treatment improved motor deficits associated with the insult that was demonstrated as an increase in distance travelled by 8.2-and 9.8-folds, mean speed by 4.6-and 5.3-folds, and rearing frequency by 8.8-and 9.4-folds in OFT as well as fall-off latency by10.7-and 15-folds in rotarod test together with a decrease in time immobile (44- and 49 %) in OFT, respectively relative to EAE mice. Additionally, nicorandil and carvedilol markedly decreased foot fault percentage (71- and 74 %) respectively in grid walk test, along with significant increase in stride length by 1.5-folds and stride width by 1.4-folds respectively in footprint test, as compared to EAE mice.

3.3. Effect of nicorandil and carvedilol on histopathological impairments in EAE mice

Demyelination and atrophy of the corpus callosum are a prominent pathological feature of MS as it is the main fiber tract in the brain involved in the performance of complex tasks, such as sensory integration and cognition [29]. Corpus callosum changes were assessed using haematoxylin and eosin (H&E; Fig. 4) as well as Luxol fast blue (LFB; Fig. 5) to evaluate the neuroprotective effect of both nicorandil and carvedilol on EAE-induced demyelination of corpus callosum. Control samples **(**Fig. 4**A-C)** demonstrated normal organized histological structures of corpus callosum region (black arrow) with abundant records of dense backed myelinated nerve fibers as observed in LFB stain, besides normally organized oligodendrocytes (blue arrow) were detected. On the contrary, EAE mice **(**Fig. 4**D)** showed focal disorganized demyelinated nerve fibers with significant vacuolization and higher inter axonal spaces in rostral body zone (dashed arrow) of corpus callosum, evidenced by a 35 % decrease in percentage area of LFB myelinated nerve fibers, relative to control. In addition, significant oligodendrocytic loss was observed with higher records of reactive microglial infiltrates (red arrow). Interestingly, nicorandil-treated mice **(**Fig. 4**E)** showed significant improvement and protective efficacy with remarkable higher records of remyelinated nerve fibers (black arrow), manifested by 1.5-folds increase in LFB myelinated nerve fibers, as compared to EAE group. In addition, an increase in oligodendrocytic populations (blue arrow) with minimal reactive microglial infiltrates were recorded. Similarly, carvedilol treatment **(**Fig. 4**F)** showed the same protective effect as nicorandil with even more enhanced remyelination process, witnessed by 1.6-folds increase in LFB myelinated nerve fibers, as compared to the insult in addition to higher records of microglial infiltrates were detected (red arrow).

3.4. Effect of nicorandil and carvedilol on MBP immunoreactivity in EAE mice

Myelin basic protein (MBP) plays a vital role in the structure and signalling of myelin and oligodendrocytes [31]. Control sections showed normal distribution of MBP, whereas EAE mice demonstrated a significant decrease in the MBP immunoexpression (46 %) in corpus callosum, when comparing to control group. Otherwise, sections taken from corpus callosum of nicorandil, and carvedilol treated mice demonstrated an obvious increase in MBP immunoreactivity by 2-and 1.9-folds respectively comparative to EAE-mice **(**Fig. 6**)**.

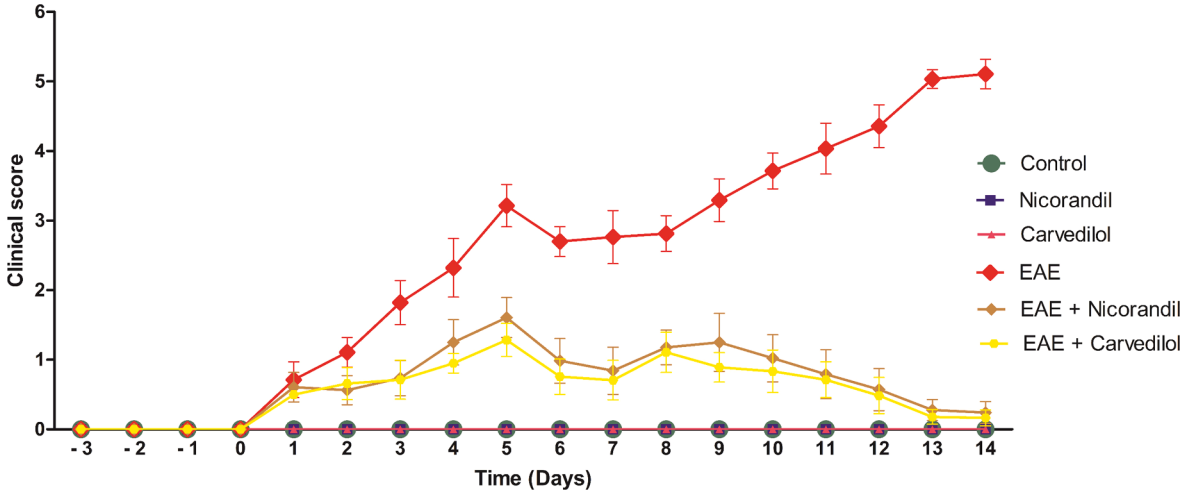

Fig. 1. Effect of Nicorandil and Carvedilol on EAE induced changes in clinical score. Data are presented as mean ± SD of 12 mice per group, using two-way ANOVA followed by Bonferroni post hoc test; $p < 0.05$. EAE; Experimental autoimmune encephalomyelitis.

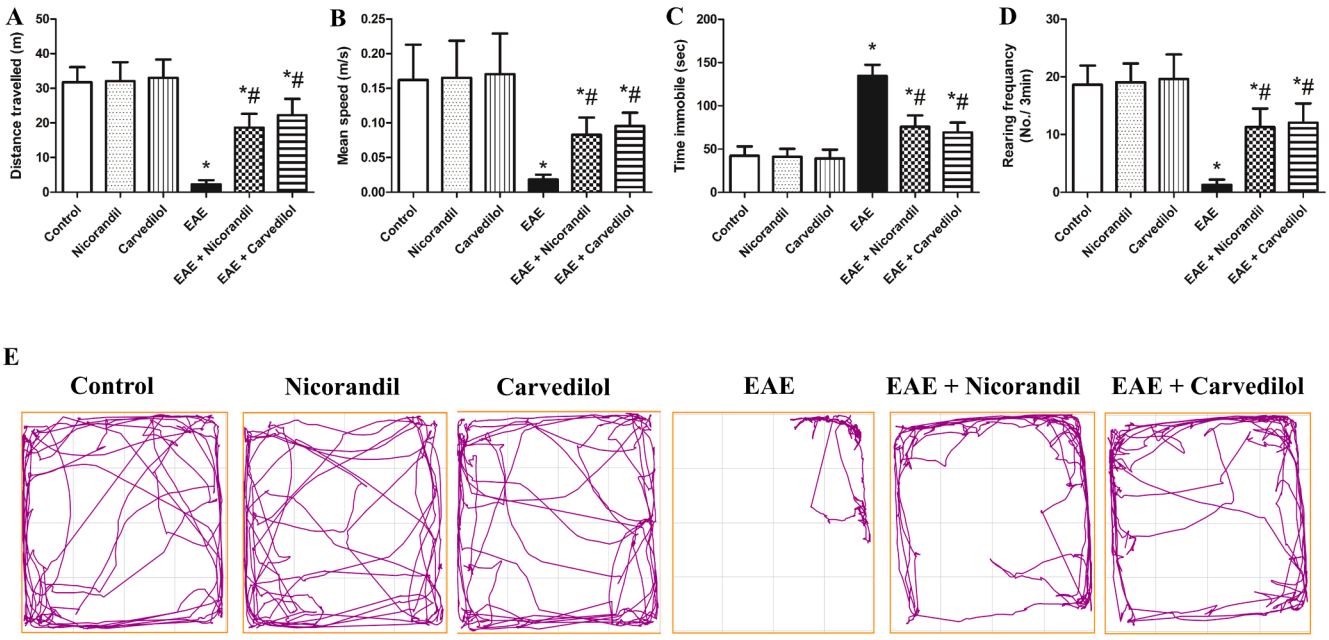

Fig. 2. Effect of Nicorandil and Carvedilol on EAE induced changes in (A) distance travelled (B) mean speed (C) time immobile (D) rearing frequency and (E) number of line crossings in Open field test as well as (F) representative track plots of mice during the test. Data are presented as mean ± SD of 12 mice per group, using one-way ANOVA followed by Tukey's post hoc test; $p < 0.05$. * vs control, # vs EAE. EAE; Experimental autoimmune encephalomyelitis.

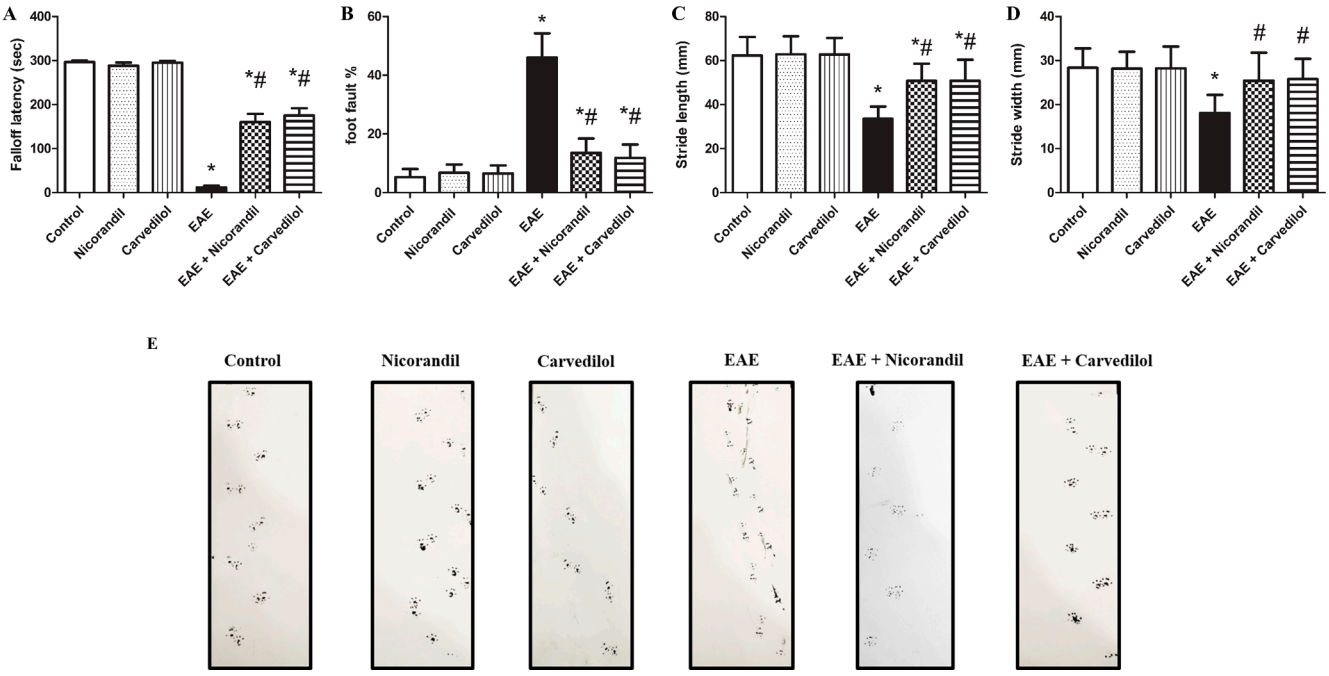

Fig. 3. Effect of Nicorandil and Carvedilol on EAE induced changes in (A) fall off latency in rotarod test, (B) Foot fault % in grid walk task, as well as (C) Stride length, (D) Stride width and (E) representative footprints of each group in Footprint test. Data are presented as mean ± SD of 12 mice per group, using one-way ANOVA followed by Tukey's post hoc test; $p < 0.05$. * vs control, # vs EAE. EAE; Experimental autoimmune encephalomyelitis.

3.5. Effect of nicorandil and carvedilol on TLR4, MyD88, TRAF6, p38 (pT180/Y182)-MAPK and (pT183/Y185)-JNK in EAE mice

In Fig. 7, EAE showed significant increase in the protein expressions of TLR4, MyD88, TRAF6, p-p38-MAPK and p-JNK by 5.5, 6.5, 4.7, 7.4 and 4.5-folds respectively compared to control mice. Oppositely, nicorandil and carvedilol succeeded to inhibit the activation of TLR4 signal transduction and reversed the aforementioned parameters, as compared to EAE-group.

3.6. Effect of nicorandil and carvedilol on neuroinflammatory markers in EAE mice

EAE demonstrated a significant elevation in neuroinflammatory markers, namely NF-κB, IL-6, IL-1β, and TNF-α, with corresponding increases of 2.2, 3.94, 3.79, and 3.59 compared to the control group. On the contrary, nicorandil and carvedilol reversed EAE-induced inflammatory status through decreasing the protein contents of NF-κB (38- and 42 %), IL-6 (47- and 50 %), IL-1β (45- and 49 %) and TNF-α (45- and 49

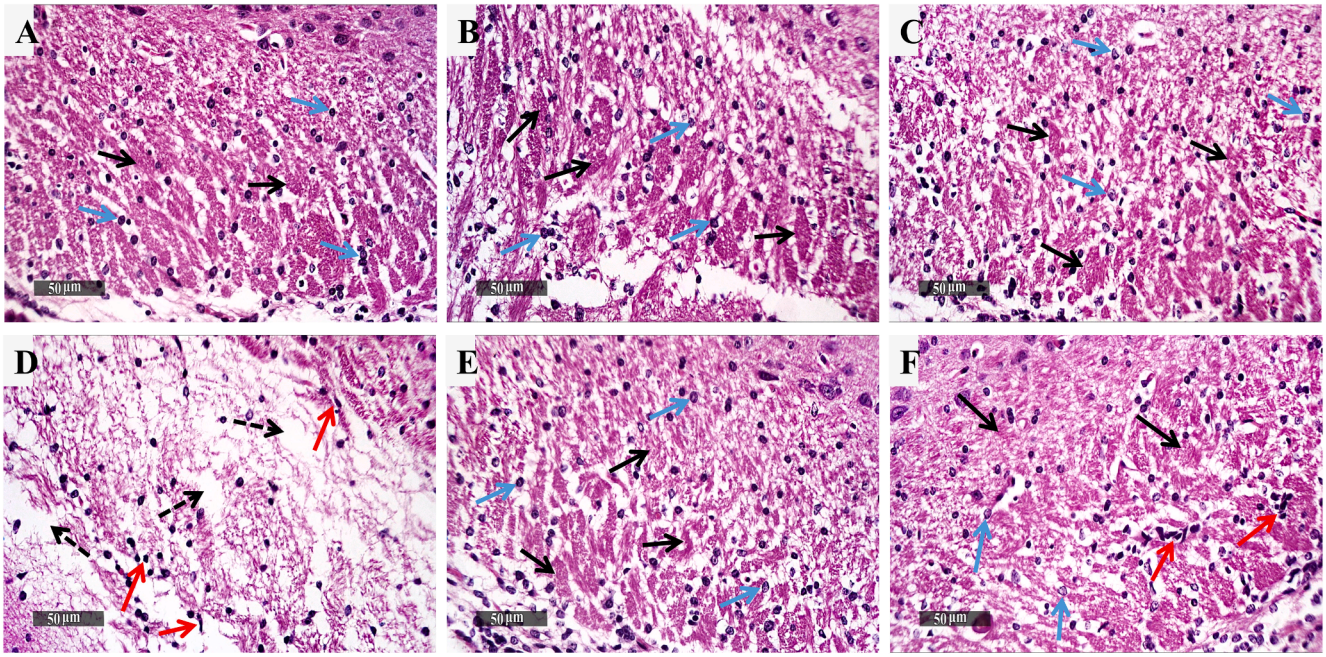

Fig. 4. Effect of Nicorandil and Carvedilol on EAE induced histopathological alterations. A-F photomicrographs represent staining of corpus callosum with H&E (Scale bar 50). **[A]** Control group, **[B]** Nicorandil alone treatment, **[C]** Carvedilol alone treatment, **[D]** EAE group, **[E]** Nicorandil treated group and **[F]** Carvedilol treated group. Well organized histological structures of corpus callosum region **(black arrow)**, normal organized oligodendrocytes **(blue arrow)**, focal disorganized demyelinated nerve fibers **(dashed arrow)**, and oligodendrocytic loss with higher records of reactive microglial infiltrates **(red arrow)**. EAE; Experimental autoimmune encephalomyelitis. (For interpretation of the references to colour in this figure legend, the reader is referred to the web version of this article.)

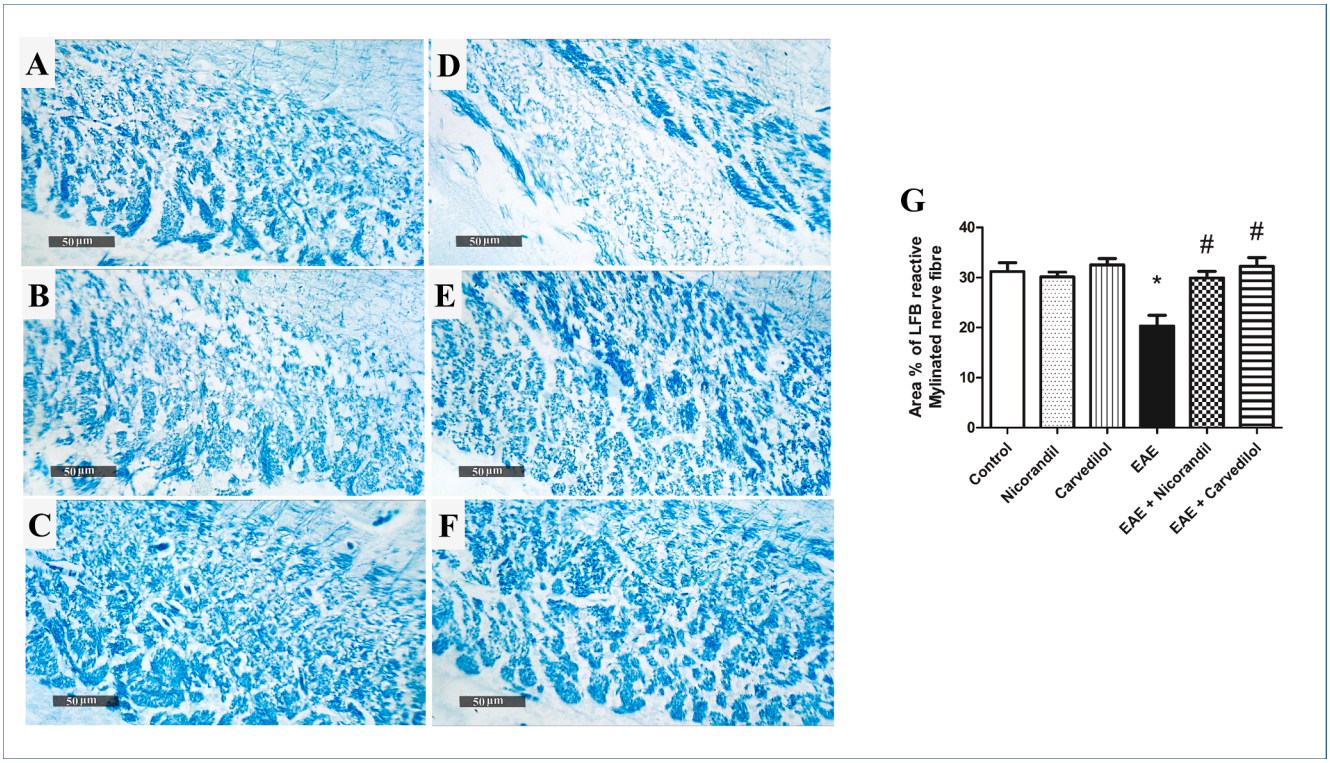

Fig. 5. Effect of Nicorandil and Carvedilol on EAE induced nerve fiber demyelination. A-F photomicrographs represent Luxol Fast Blue (LFB) staining of myelinated nerve fibers in Corpus Callosum (Scale bar 50). **[A]** Control group, **[B]** Nicorandil alone treatment, **[C]** Carvedilol alone treatment, **[D]** EAE group, **[E]** Nicorandil treated group, **[F]** Carvedilol treated group and **[G]** Area % of LFB reactive myelinated nerve fiber. Data are presented as mean ± SD of 3 mice per group, using one-way ANOVA followed by Tukey's post hoc test; $p < 0.05$. * vs control, # vs EAE. EAE; Experimental autoimmune encephalomyelitis. (For interpretation of the references to colour in this figure legend, the reader is referred to the web version of this article.)

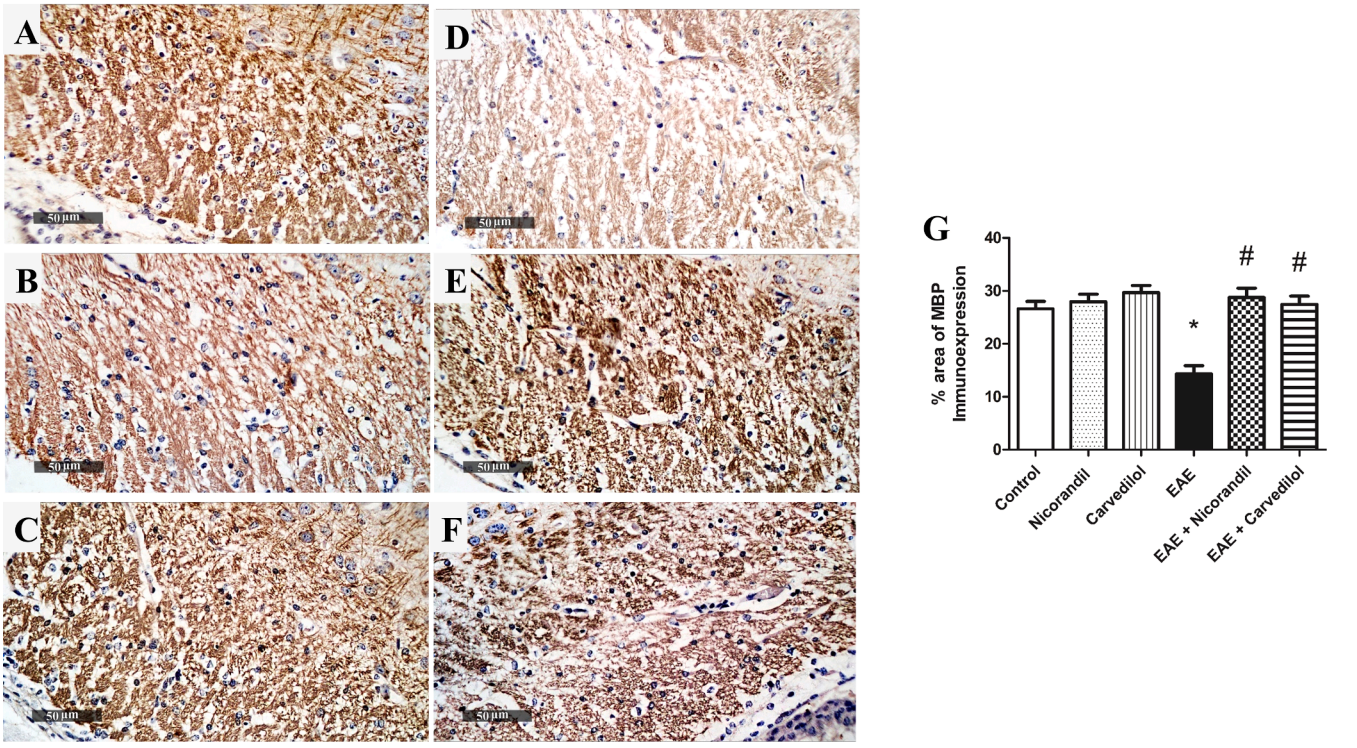

Fig. 6. Effect of Nicorandil and Carvedilol on EAE induced changes in MBP immunoreactivity. A-F photomicrographs represent immunohistochemical staining of MBP in Corpus Callosum (Scale bar 50). [A] Control group, **[B]** Nicorandil alone treatment, **[C]** Carvedilol alone treatment, **[D]** EAE group, **[E]** Nicorandil treated group, **[F]** Carvedilol treated group and **[G]** % area of MBP immunoexpression. Data are presented as mean ± SD of 3 mice per group, using one-way ANOVA followed by Tukey's post hoc test; $p < 0.05$. * vs control, # vs EAE. EAE; Experimental autoimmune encephalomyelitis.

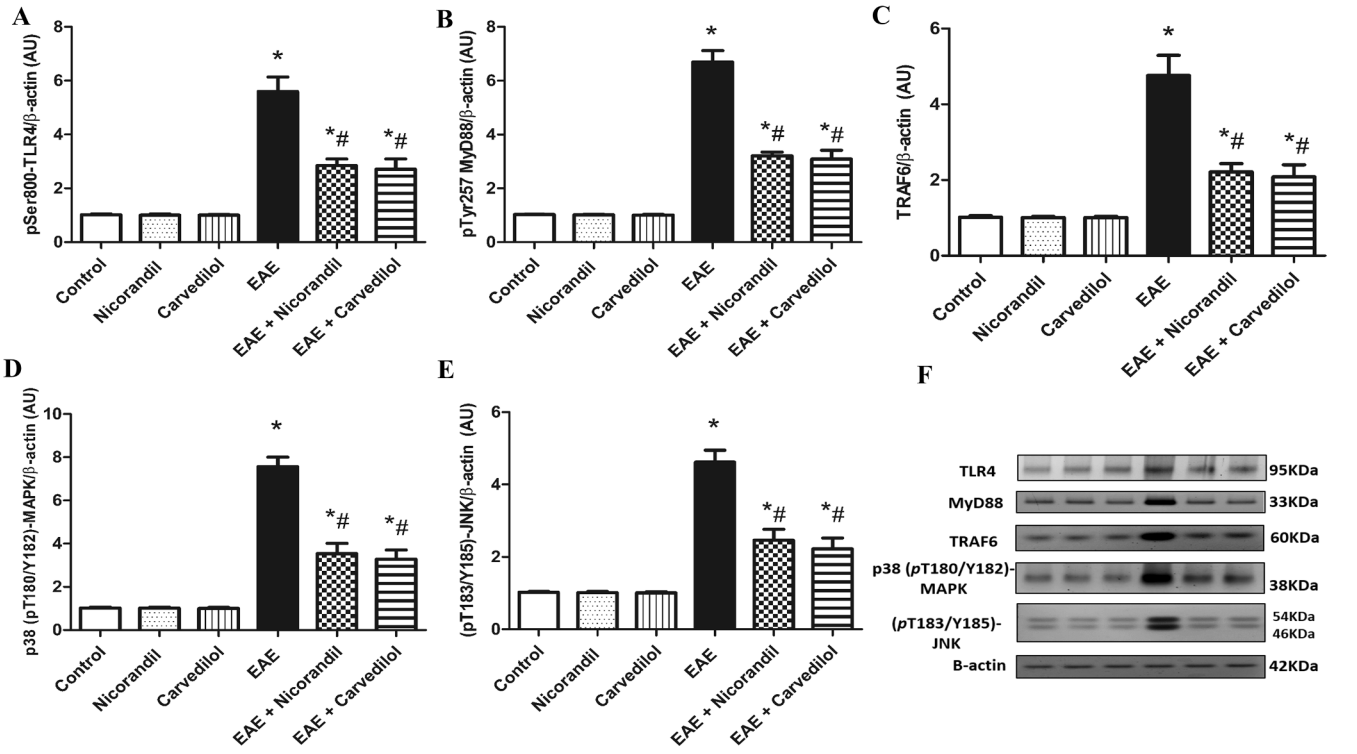

Fig. 7. Effect of Nicorandil and Carvedilol on EAE induced alteration in protein expression of (A) TLR4, (B) MyD88, (C) TRAF6, (D) (pT183/Y185)-JNK, (E) p38 (pT180/Y182)-MAPK and (F) Western blot for [TLR4, MyD88, TRAF6, (pT183/Y185)-JNK, p38 (pT180/Y182)-MAPK and β-actin] for different groups. Data are presented as mean ± SD of 3 mice per group, using one-way ANOVA followed by Tukey's post hoc test; $p < 0.05$. * vs control, # vs EAE. EAE; Experimental autoimmune encephalomyelitis.

%), as compared to EAE mice (Fig. 8).

3.7. Effect of nicorandil and carvedilol on immunopathological status in EAE mice

EAE induced immunopathological status manifested as an increase in CD4, TGF-β, IL-17 gene expression by 6.5, 5.5 and 6.2-folds, respectively as well as TGF-β, IL-17 and IL-23 contents by 3.9, 4.7 and 2-folds, respectively relative to control group. Contrariwise, treatment with nicorandil and carvedilol demonstrated an immunomodulating effect that was witnessed as a decline in the gene expression of CD4 (62 %), TGF-β (48 %) and IL-17 (50 %) as well as the contents of TGF-β (50 %), IL-17 (53 %) and IL-23 (37 %), as compared to EAE mice (Fig. 9).

3.8. Effect of nicorandil and carvedilol on oxidative stress status in EAE mice

EAE exacerbated oxidative stress status that was witnessed as a significant decrease in Nrf2 content and SOD activity (56 %) as well as increase in MDA content by 2.9-folds compared to control group. On the other hand, nicorandil and carvedilol treatment markedly increase both Nrf2 content by 1.9-folds and SOD activity by 2-folds respectively, in addition to significant decrease in MDA content (53 %) as compared to EAE mice (Fig. 10).

3.9. Effect of nicorandil and carvedilol on Bax, Bcl-2 and Caspase-3 in EAE mice

EAE manifested a significant increase in Bax protein expression by 3.6-folds as well as caspase-3 gene expression by 8.3-folds, along with decline in Bcl-2 protein expression (81 %), as compared to control group. In opposition, nicorandil and carvedilol succeeded to inhibit apoptotic influx and decreased Bax protein expression (56- and 60 %) as well as caspase-3 gene expression (52- and 53 %), together with increment in Bcl-2 protein expression by 4-folds respectively, as compared to EAE mice (Fig. 11).

4. Discussion

The present study establishes the potential neuroprotective effects of nicorandil and carvedilol against EAE-induced multiple sclerosis in a mouse model. This conclusion is supported by a range of observed effects, including the improvement of clinical signs and motor impairment, the suppression of the TLR4/MyD88/TRAF6 signalling cascade with downstream inhibition of the JNK/p38-MAPK axis, reduction of inflammatory markers (NF-κB p65, TNF-α, IL-1β, and IL-6), alleviation

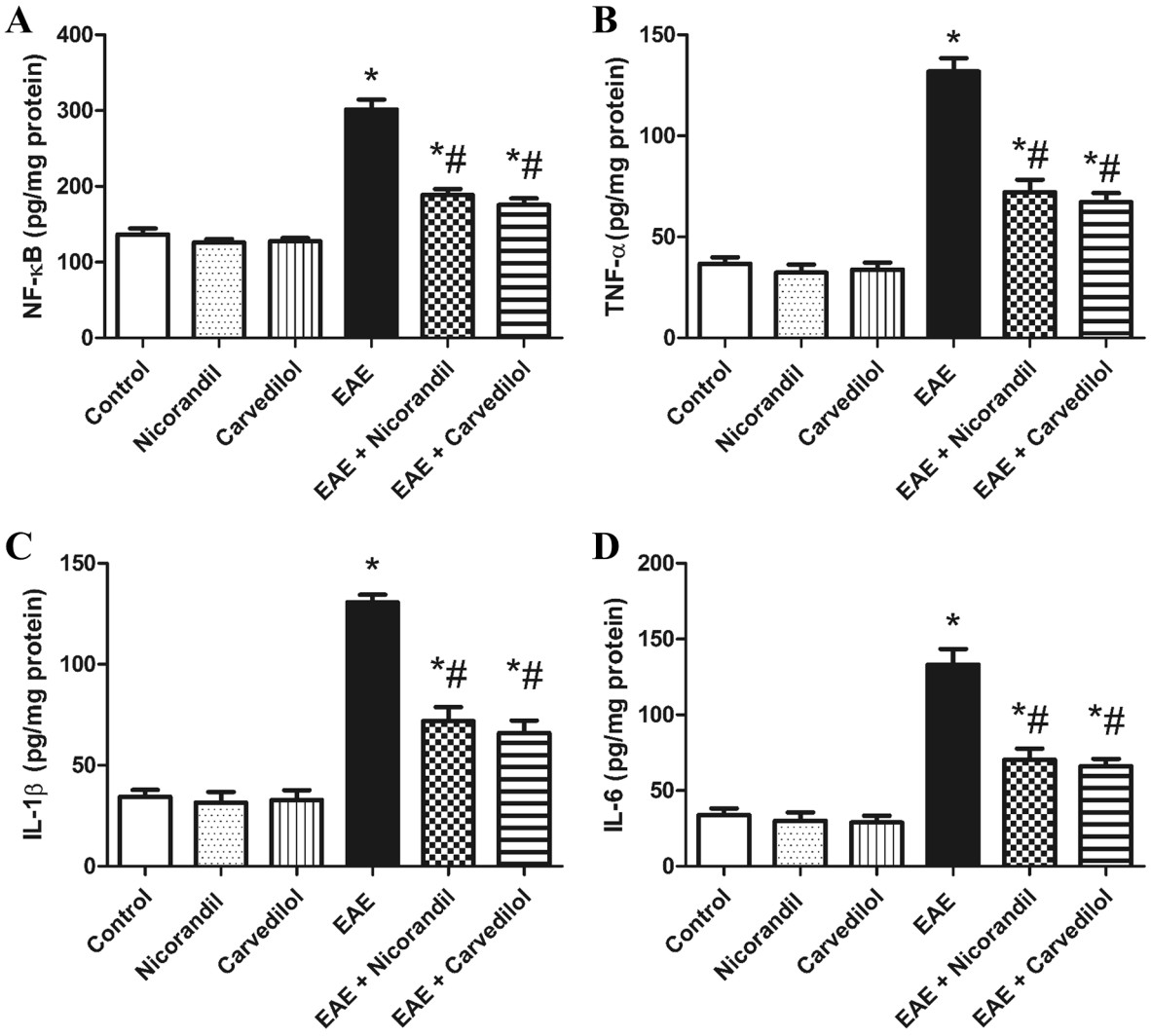

Fig. 8. Effect of Nicorandil and Carvedilol on EAE induced alteration in the contents of (A) NF-κB p65, (B) TNF-α, (C) IL-1β and (D) IL-6. Data are presented as mean ± SD of 6 mice per group, using one-way ANOVA followed by Tukey's post hoc test; $p < 0.05$. * vs control, # vs EAE. EAE; Experimental autoimmune encephalomyelitis.

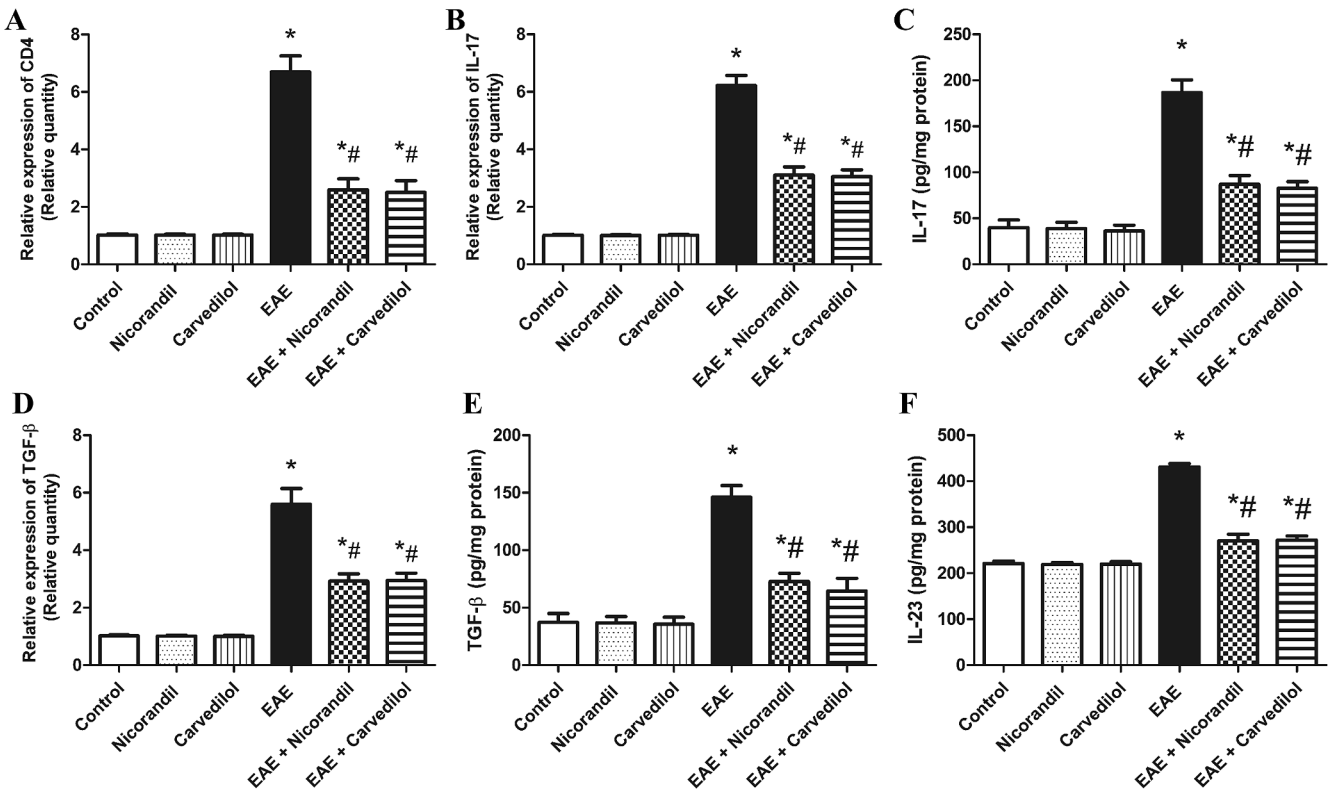

Fig. 9. Effect of Nicorandil and Carvedilol on EAE induced alteration in (A) CD4 gene expression, (B) IL-17 gene expression, (C) IL-17 content, (D) TGF-β gene expression, (E) TGF-β content and (F) IL-23 content. Data are presented as mean ± SD of 6 mice per group, using one-way ANOVA followed by Tukey's post hoc test; $p < 0.05$. * vs control, # vs EAE. EAE; Experimental autoimmune encephalomyelitis.

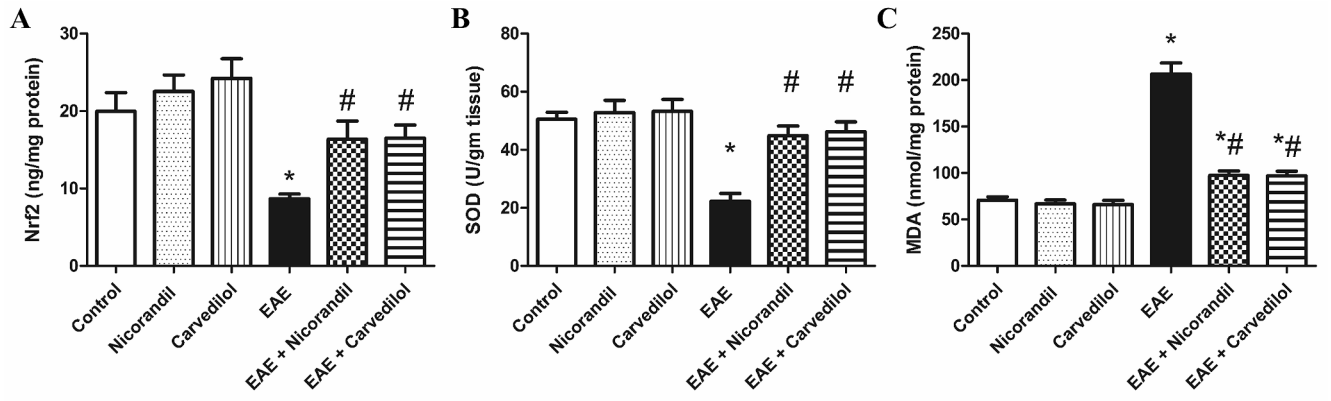

Fig. 10. Effect of Nicorandil and Carvedilol on EAE induced alteration in (A) Nrf2 content, (B) SOD activity, and (C) MDA content. Data are presented as mean ± SD of 6 mice per group, using one-way ANOVA followed by Tukey's post hoc test; $p < 0.05$. * vs control, # vs EAE. EAE; Experimental autoimmune encephalomyelitis.

of oxidative stress, immunomodulation, and inhibition of apoptotic flux.

In MS, extensive glia activation in brain and spinal cord results in release of pro-inflammatory cytokines and chemokines which leads to significant alteration of neuronal signalling, resulting in multifocal demyelination and axonal loss, that consequently causes a wide range of motor, cognitive, and sensory symptoms [38]. Previous studies demonstrated the role of EAE in glial activation and neurodegeneration that lead to sever motor abnormalities raising the contribution of microglia in mediating motor disorder in CNS [39,40]. Indeed, EAE has been proven to cause primary demyelination of axonal tracks, impaired axonal conduction in the CNS [41] together with, ascending paralysis beginning in the tail and hind limbs and progressing to the forelimbs in animals, as reported herein and previously [42]. Moreover, open field, rotarod, grid walk and footprint tests were used to evaluate the motor and behavioural abnormalities induced by EAE. Noteworthy, nicorandil and carvedilol treatment attenuated behavioural abnormalities induced by EAE and showed obvious improvement in motor incoordination, locomotor activity, grip strength.

Toll like receptor 4 (TLR4) is widely acknowledged to be activated in autoimmune disorders [43] and its activation results in expression of various inflammatory cytokines, leading to persistent inflammation and tissue damage [44]. Myeloid differentiation 88 MyD88 is an adaptor protein that links TLRs to its downstream molecules [45]. The involvement of the TLR-MyD88 signalling pathway in the pathogenesis of neurological disorders such as MS has been reported [46]. In EAE, $DAMP_S$ such as HMGB1 are released from ongoing inflammation,

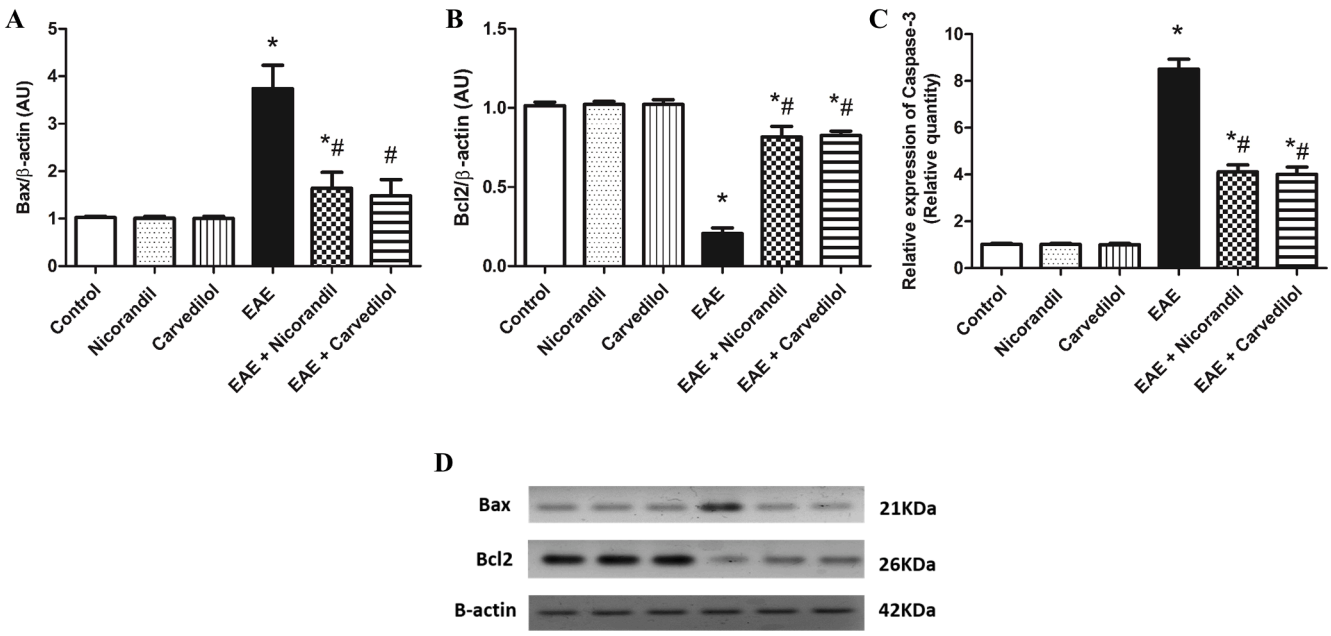

Fig. 11. Effect of Nicorandil and Carvedilol on EAE induced alteration in the protein expression of (A) Bax, and (B) Bcl-2, as well as (C) Caspase-3 gene expression and (D) Western blot for (Bax, Bcl-2 and β-actin) for different groups. Data are presented as mean ± SD of 3–6 mice per group, using one-way ANOVA followed by Tukey's post hoc test; $p < 0.05$. * vs control, # vs EAE. EAE; Experimental autoimmune encephalomyelitis.

demyelination and breakdown products and binds to TLRs that are expressed in microglia, astrocytes and neurons [47]. When TLRs recognize DAMPs, the death domains of both MyD88 and IL-1 receptor-associated kinase-4 (IRAK-4) interact and form the MyD88-IRAK-4 complex, which induces the phosphorylation of IRAKs. Afterwards, IRAKs interact with TRAF6 which promotes TGF-β activated kinase-1 (TAK-1) and TAK1-binding proteins (TABs) activation after leaving MyD88 [48]. TABs elicit NF-κB signalling pathway through the phosphorylation of I-kB (IkB), which results in its ubiquitylation and degradation. This degradation subsequently permits NF-κB to be released and translocated to the nucleus [49,50]. Moreover, TAK-1 can activate JNK and P38-MAPK, triggering a positive feed forward inflammatory cycle [48].

Noteworthy, nicorandil activates ATP-dependant potassium (K_{ATP}) channels both directly and indirectly by a NO-cGMP mediated mechanism [44], that result in reducing the expression and release of inflammatory mediators from both macrophages and microglia. Indeed, nicorandil reduced the protein expression of TLR4 and its downstream target proteins as reported herein.

In the same context, nicorandil exerted a neuroprotective effect against cerebral ischemia and neurodegenerative conditions *via* opening K_{ATP} channels [51,52]. Noteworthy, activation of K_{ATP} causes inhibition of HMGB1-induced TLR4/MyD88/NF-κB signalling transduction [53]. Additionally, K_{ATP} regulates neuronal activities, specifically synaptic plasticity processes that are essential for memory formation [54]. Notably, nicorandil produced an anti-inflammatory effect against rheumatoid arthritis *via* inhibiting TLR4/MyD88 signalling pathway [44], thus activation of K_{ATP} channels could be a promising therapeutic agent to guard against neuroinflammation induced by TLR4 activation.

Carvedilol, an antihypertensive drug with non-selective β receptor and α_1 receptor blocking effect, has antioxidant, anti-inflammatory and neuroprotective effects [55]. In the current study, carvedilol inhibited TLR4 activation and the downstream signal transduction; effects that could be attributed to metal chelating and free radical scavenging abilities of carvedilol [56], where the antioxidant activity of carvedilol comes from the carbazole moiety [57]. Noteworthy, ROS overproduction creates oxidative stress status that results in release of DAMPs and activation of TLR4 which have been implicated in demyelination and axonal damage in EAE [58,59]. In the same context, carvedilol reduced the expression of TLR4 and its subsequent signalling cascade in the hepatic tissues of rats with cholestatic liver fibrosis [27].

NF-κB is a transcription factor that plays a vital role in inflammatory response, and its activation contributes to the pathogenic processes of various inflammatory diseases [60]. In EAE, activation of TLR4/MyD88/TRAF6 signalling pathway stimulates NF-κB that stimulates the synthesis of pro-inflammatory cytokines. [10]. Inflammatory cytokines including IL-6, IL-1β and TNF-α produced by microglia activation are important in the pathogenesis of MS and critical for EAE development [61], particularly in the early stages causing immune system activation and destruction of oligodendrocytes and myelin [62]. Indeed, those inflammatory cytokines and co-stimulatory molecules expression in macrophages were inhibited by downregulating NF-κB pathway activity [63]. Interestingly, pre-treatment with nicorandil decreased IL-6 and TNF-α production as reported herein and previously in kidney ischaemia–reperfusion injury [64], in addition to reduction of IL-1β; effects could be attributed to supressing NF-κB activity. Furthermore, carvedilol showed marked reduction in IL-1β and TNF-α secretion as reported herein and in experimental autoimmune myocarditis (EAM) [65]. Noteworthy, activation of β-adrenergic receptors within CNS enhances inflammation *via* increasing the expression of IL-1β [66], consequently blocking of β-adrenergic receptors using carvedilol inhibits IL-1β. In parallel, inhibiting NF-κB activity could be another reason for decreasing IL-1β, IL-6 and TNF-α.

Concerning immunopathological alteration, activation of TLR4 augments the proliferation and viability of CD4+ T cells [13]. Indeed, cluster of differentiation 4 ($CD4^+$) T cells are essential for immune responses regulation by secreting cytokines that regulate various cellular functions [67]. A previous study demonstrated the contribution of $CD4^+$ T cells in demyelination, inflammation, disability and disease progression in animal model of MS *via* interleukin-17 (IL-17) production [68,69]. Moreover, strong immunoreactivity of Transforming growth factor-beta (TGF-β), an important injury-response factor and modulator of immune responses, was observed in the CNS of EAE mice [70]. Notably, inhibition of TGF-β signalling reduced the accumulation of T cells in the CNS leading to amelioration of EAE progression [71]. In addition to TGF-β, IL-23 is a crucial factor for EAE induction through its

contribution in the differentiation and propagation of T helper 17 (Th17) [72,73]. Furthermore, in EAE mice, IL-23 promotes the expansion of a subpopulation of Th cells that express cytokines IL-17, IL-6, and TNF-α specifically [74]. Of interest, IL-17 has been implicated in various models for autoimmune diseases such as the animal model for MS [75]. In mice with EAE knocking out either IL-17 or IL-23 abrogated the disease [76]. In the current study, nicorandil and carvedilol supressed the expression of $CD4^{+}$, TGF-β, IL-17 and IL-23 through inhibiting TLR4/MyD88 signalling, indicating the immunomodulatory effect against EAE.

Several studies reported the crucial role of ROS in myelin phagocytosis and pathogenesis of MS [77,78]. Indeed, ROS and reactive nitrogen species (RNS) produced during the inflammatory response, leads to monocyte interactions with brain endothelium, causing loss of blood–-brain barrier integrity and tight-junction alterations [79]. Furthermore, oxidative stress has been linked to mitochondrial injury and energy failure, which could explain some of the pathological features of multiple sclerosis, such as demyelination, oligodendrocyte apoptosis, and astrocyte dysfunction [80]. In addition, marked elevated level of oxidants has been found in serum and cerebrospinal fluid of rodent induced by EAE [81]. A previous study has demonstrated the role of Nrf2 improvement in preventing the effect of oxidative stress *via* scavenging ROS and promoting the expression of antioxidants enzymes such as SOD and glutathione peroxidase [82]. Of note, suppression of SOD activity aggravated tissue injury in an EAE mouse model, whereas injury and disability was reduced after SOD enhancement [83]. Furthermore, it has been reported that inhibiting MDA ameliorates neurological deficits in a rodent model of EAE [84]. Herein, nicorandil and carvedilol showed antioxidant activity against oxidative stress induced by EAE *via* elaboration of Nrf2 that led to increase in SOD activity and reduction of MDA content. Also, the inhibition of NF-κB activity could be another reason for increasing Nrf2 content as reported herein and previously [85].

Several CNS disorders have been linked to imbalance in Bax/Bcl-2/caspase-3 apoptotic signalling cascade [86]. Indeed, Bcl-2 and Bax proteins are members of Bcl-2 family that control apoptosis *via* regulating numerous mitochondrial functions [81]. Bcl-2 is one of the most vital pro-survival proteins, whereas Bax is a crucial mediator of apoptosis, so controlling apoptosis requires a delicate balance between pro- and anti-apoptotic proteins [81]. Moreover, cysteine-aspartic proteases-3 (Caspase-3), a key enzyme in apoptosis, is involved in neuronal death and was significantly increased in EAE mice model and inhibiting its activation plays a neuroprotective role in MS [88]. In the current study, a significant increase in Bax protein expression as well as caspase gene expression along with reduction in Bcl-2 protein expression was demonstrated in EAE mice, that play a vital role in initiation of apoptotic flux as observed herein and previously [87]. Furthermore, oxidative stress causes downregulation of Bcl-2 which contributes to apoptotic cascade activation and accelerates the death process following EAE induction [81]. In parallel, the stress-activated MAPK pathway not only plays a clear role in the process of inflammation but also enhances apoptotic cascades in the presence of excessive oxidative stress [89]. The translocation of cytoplasmic JNK to the nucleus can be triggered by oxidative stress, resulting in the subsequent production of the pro-apoptotic protein Bax and the effector caspase-3 [90]. In addition, the activation of p38-MAPK is necessary for the translocation of Bax protein into the mitochondria and subsequent release of cytochrome *c* [91]. It has been reported that nicorandil and carvedilol can regulate Bcl-2/Bax/caspase-3 apoptotic signalling in cardiac myocytes and testicular tissues respectively [92,93]. Similarly, in the present study, nicorandil and carvedilol increased Bcl-2 expression concomitant with decrease in both Bax and caspase-3 expression.

In conclusion, the current study demonstrates for the first time the role of TLR4/MyD88/ TRAF6/JNK/p-38MAPK/NF-κB p65 pathway inhibition and Bcl-2 upregulation in the neuroprotective and anti-inflammatory effect of nicorandil and carvedilol against EAE induced neuronal loss, which might offer a new potentiality for the possible role of anti-ischemic drugs in treating MS.

Funding

There were no dedicated financial support awarded to this research by public, commercial, or not-for-profit funding agencies.

CRediT authorship contribution statement

Aya M. Mustafa: Conceptualization, Methodology, Investigation, Formal analysis, Writing – original draft. **Aya M. Shaheen:** Software, Validation, Writing – review & editing. **Hala F. Zaki:** Data curation, Supervision. **Mostafa A. Rabie:** Conceptualization, Methodology, Writing – review & editing, Visualization, supervision.

Declaration of competing interest

The authors declare that they have no known competing financial interests or personal relationships that could have appeared to influence the work reported in this paper.

Data availability

Data will be made available on request.

References

[1] Z. Fonseca-Kelly, M. Nassrallah, J. Uribe, R.S. Khan, K. Dine, M. Dutt, K.S. Shindler, Resveratrol neuroprotection in a chronic mouse model of multiple sclerosis, Front. Neurol. 3 (2012) 84, https://doi.org/10.3389/fneur.2012.00084.
[2] S. Glatigny, E. Bettelli, Experimental autoimmune encephalomyelitis (EAE) as animal models of multiple sclerosis (MS), Cold Spring Harb Perspect Med. (2018) a028977, https://doi.org/10.1101/cshperspect.a028977.
[3] N. Khan, M.T. Smith, Multiple sclerosis-induced neuropathic pain: pharmacological management and pathophysiological insights from rodent EAE models, Inflammopharmacology 22 (1) (2014) 1–22, https://doi.org/10.1007/s10787-013-0195-3.
[4] Y.H. Jeong, W. Li, Y. Go, Y.-C. Oh, Atractylodis rhizoma alba attenuates neuroinflammation in BV2 microglia upon LPS stimulation by inducing HO-1 activity and inhibiting NF-κB and MAPK, Int. J. Mol. Sci. 20 (2019) 4015, https://doi.org/10.3390/ijms20164015.
[5] S.-S. Zhang, M. Liu, D.-N. Liu, Y.-L. Yang, G.-H. Du, Y.-H. Wang, TLR4-IN-C34 inhibits lipopolysaccharide-stimulated inflammatory responses via downregulating TLR4/MyD88/NF-κB/NLRP3 signaling pathway and reducing ROS generation in BV2 cells, Inflammation (2022) 1–13, https://doi.org/10.1007/s10753-021-01588-8.
[6] A.M. Mustafa, M.A. Rabie, H.F. Zaki, A.M. Shaheen, Inhibition of Brain GTP Cyclohydrolase I Attenuates 3-Nitropropionic Acid-Induced Striatal Toxicity: Involvement of Mas Receptor/PI3k/Akt/CREB/BDNF Axis, Front. Pharmacol. 12 (2021), 740966, https://doi.org/10.3389/fphar.2021.740966.
[7] D. Erny, A.L. Hrabě de Angelis, D. Jaitin, P. Wieghofer, O. Staszewski, E. David, H. Keren-Shaul, T. Mahlakoiv, K. Jakobshagen, T. Buch, Host microbiota constantly control maturation and function of microglia in the CNS, Nat. Neurosci. 18 (2015) 965–977, https://doi.org/10.1038/nn.4030.
[8] I. Glezer, A. Simard, S. Rivest, Neuroprotective role of the innate immune system by microglia, Neuroscience 147 (2007) 867–883, https://doi.org/10.1016/j.neuroscience.2007.02.055.
[9] P.L. Nguyen, B.P. Bui, H. Lee, J. Cho, A novel 1, 8-naphthyridine-2-carboxamide derivative attenuates inflammatory responses and cell migration in LPS-treated BV2 cells via the suppression of ROS generation and TLR4/Myd88/NF-κB signaling pathway, Int. J. Mol. Sci. 22 (2021) 2527, https://doi.org/10.3390/ijms22052527.
[10] Y. Chu, Y. Jing, X. Zhao, M. Wang, M. Zhang, R. Ma, W. Ma, Y. Lv, L. Zhu, Modulation of the HMGB1/TLR4/NF-κB signaling pathway in the CNS by matrine in experimental autoimmune encephalomyelitis, J. Neuroimmunol. 352 (2021), 577480, https://doi.org/10.1016/j.jneuroim.2021.577480.
[11] T. Kawai, S. Akira, The role of pattern-recognition receptors in innate immunity: update on Toll-like receptors, Nat. Immunol. 11 (2010) 373–384, https://doi.org/10.1038/ni.1863.
[12] M. Li, D. Zhang, X. Ge, X. Zhu, Y. Zhou, Y. Zhang, X. Peng, A. Shen, TRAF6-p38/JNK-ATF2 axis promotes microglial inflammatory activation, Exp. Cell Res. 376 (2019) 133–148, https://doi.org/10.1016/j.yexcr.2019.02.005.
[13] J.M. Reynolds, G.J. Martinez, Y. Chung, C. Dong, Toll-like receptor 4 signaling in T cells promotes autoimmune inflammation, PNAS 109 (2012) 13064–13069, https://doi.org/10.1073/pnas.1120585109.
[14] Y. Liu, C. Zhao, J. Meng, N. Li, Z. Xu, X. Liu, S. Hou, Galectin-3 regulates microglial activation and promotes inflammation through TLR4/MyD88/NF-kB in experimental autoimmune uveitis, Clin. Immunol. 236 (2022), 108939, https://doi.org/10.1016/j.clim.2022.108939.

[15] C. Zheng, J. Chen, F. Chu, J. Zhu, T. Jin, Inflammatory role of TLR-MyD88 signaling in multiple sclerosis, Front. Mol. Neurosci. 12 (2020) 314, https://doi.org/10.3389/fnmol.2019.00314.

[16] C.G. Nichols, KATP channels as molecular sensors of cellular metabolism, Nature 440 (2006) 470–476, https://doi.org/10.1038/nature04711.

[17] A. Thomzig, M. Wenzel, C. Karschin, M.J. Eaton, S.N. Skatchkov, A. Karschin, R. W. Veh, Kir6. 1 is the principal pore-forming subunit of astrocyte but not neuronal plasma membrane K-ATP channels, Mol. Cell Neurosci. 18 (2001) 671–690, https://doi.org/10.1006/mcne.2001.1048.

[18] F. Zhou, H.H. Yao, J.Y. Wu, J.H. Ding, T. Sun, G. Hu, Opening of microglial KATP channels inhibits rotenone-induced neuroinflammation, J. Cell Mol. Med. 12 (2008) 1559–1570, https://doi.org/10.1111/j.1582-4934.2007.00144.x.

[19] Y.F. Dong, L.X. Wang, X. Huang, W.J. Cao, M. Lu, J.H. Ding, X.L. Sun, G. Hu, Kir6. 1 knockdown aggravates cerebral ischemia/reperfusion-induced neural injury in mice, CNS Neurosci. Ther. 19 (2013) 617–624, https://doi.org/10.1111/cns.12117.

[20] A.R. Gade, M. Kang, H.I. Akbarali, Hydrogen sulfide as an allosteric modulator of ATP-sensitive potassium channels in colonic inflammation, Mol. Pharmacol. 83 (2013) 294–306, https://doi.org/10.1124/mol.112.081596.

[21] G.C. Kane, C.F. Lam, F. O'Cochlain, D.M. Hodgson, S. Reyes, X.K. Liu, T. Miki, S. Seino, Z.S. Katusic, A. Terzic, Gene knockout of the KCNJ8-encoded Kir6. 1 KATP channel imparts fatal susceptibility to endotoxemia, FASEB J. 20 (2006) 2271–2280, https://doi.org/10.1096/fj.06-6349com.

[22] S. Gupta, P. Singh, B. Sharma, Neuroprotective effects of nicorandil in chronic cerebral hypoperfusion-induced vascular dementia, J. Stroke Cerebrovasc. Dis. 25 (2016) 2717–2728, https://doi.org/10.1016/j.jstrokecerebrovasdis.2016.07.023.

[23] S. Gupta, B. Sharma, Protective effects of phosphodiesterase-1 (PDE1) and ATP sensitive potassium (KATP) channel modulators against 3-nitropropionic acid induced behavioral and biochemical toxicities in experimental Huntington′ s disease, Eur. J. Pharmacol. 732 (2014) 111–122, https://doi.org/10.1016/j.ejphar.2014.03.032.

[24] J. Xie, L. Duan, X. Qian, X. Huang, J. Ding, G. Hu, KATP channel openers protect mesencephalic neurons against MPP+-induced cytotoxicity via inhibition of ROS production, J. Neurosci. Res. 88 (2010) 428–437, https://doi.org/10.1002/jnr.22213.

[25] A.P. Zhao, Y.F. Dong, W. Liu, J. Gu, X.L. Sun, Nicorandil Inhibits Inflammasome Activation and Toll-Like Receptor-4 Signal Transduction to Protect against Oxygen-Glucose Deprivation-Induced Inflammation in BV-2 Cells, CNS Neurosci. Ther. 20 (2014) 147–153, https://doi.org/10.1111/cns.12178.

[26] K. Beattie, G. Phadke, J. Novakovic, Carvedilol, Profiles Drug Subst Excip Relat Methodol. 38 (2013) 113-157. doi: 10.1016/B978-0-12-407691-4.00004-6.

[27] X. Tian, H. Zhao, Z. Guo, Effects of Carvedilol on the Expression of TLR4 and its Downstream Signaling Pathway in the Liver Tissues of Rats with Cholestatic Liver Fibrosis, Curr. Mol. Med. 20 (2020) 708–716, https://doi.org/10.2174/1566524020666200220130705.

[28] S.I. Savitz, J.A. Erhardt, J.V. Anthony, G. Gupta, X. Li, F.C. Barone, D. M. Rosenbaum, The novel β-blocker, carvedilol, provides neuroprotection in transient focal stroke, J. Cereb. Blood Flow Metab. 20 (2000) 1197–1204, https://doi.org/10.1097/00004647-200008000-00005.

[29] M.A. Sadek, E.A. Kandil, N.S. El Sayed, H.M. Sayed, M.A. Rabie, Semaglutide, a novel glucagon-like peptide-1 agonist, amends experimental autoimmune encephalomyelitis-induced multiple sclerosis in mice: Involvement of the PI3K/Akt/GSK-3β pathway, Int. Immunopharmacol. 115 (2023), 109647, https://doi.org/10.1016/j.intimp.2022.109647.

[30] P.M. Grace, L.C. Loram, J.P. Christianson, K.A. Strand, J.G. Flyer-Adams, K. R. Penzkover, J.R. Forsayeth, A.-M. van Dam, M.J. Mahoney, S.F. Maier, Behavioral assessment of neuropathic pain, fatigue, and anxiety in experimental autoimmune encephalomyelitis (EAE) and attenuation by interleukin-10 gene therapy, Brain Behav. Immun. 59 (2017) 49–54, https://doi.org/10.1016/j.bbi.2016.05.012.

[31] T. Sullivan, N.T. Lam, M. Haberman, M.J. Beatka, M.Z. Afzal, M.W. Lawlor, J. L. Strande, Cardioprotective effect of nicorandil on isoproterenol induced cardiomyopathy in the Mdx mouse model, BMC Cardiovasc. Disord. 21 (2021) 1–12, https://doi.org/10.1186/s12872-021-02112-4.

[32] R. Nishio, T. Shioi, S. Sasayama, A. Matsumori, Carvedilol increases the production of interleukin-12 and interferon-γ and improves the survival of mice infected with the encephalomyocarditis virus, J. Am. Coll. Cardiol. 41 (2003) 340–345, https://doi.org/10.1016/s0735-1097(02)02711-0.

[33] S. Capoccia, F. Maccarinelli, B. Buffoli, L.F. Rodella, O. Cremona, P. Arosio, F. Cirulli, Behavioral characterization of mouse models of neuroferritinopathy, PLoS One 10 (2015) e0118990.

[34] Y.K. Baskin, W.D. Dietrich, E.J. Green, Two effective behavioral tasks for evaluating sensorimotor dysfunction following traumatic brain injury in mice, J. Neurosci. Methods 129 (2003) 87–93, https://doi.org/10.1016/s0165-0270(03)00212-7.

[35] K.J. Livak, T.D. Schmittgen, Analysis of relative gene expression data using real-time quantitative PCR and the 2− ΔΔCT method, Methods 25 (2001) 402–408, https://doi.org/10.1006/meth.2001.1262.

[36] A. Sidhu, V. Diwan, H. Kaur, D. Bhateja, C.K. Singh, S. Sharma, S.S. Padi, Nicotinamide reverses behavioral impairments and provides neuroprotection in 3-nitropropionic acid induced animal model ofHuntington's disease: implication of oxidative stress- poly (ADP- ribose) polymerase pathway, Metab. Brain Dis. 33 (2018) 1911–1921, https://doi.org/10.1007/s11011-018-0297-0.

[37] C.F.A. Culling, Handbook of histopathological and histochemical techniques: including museum techniques, Butterworth-Heinemann, 2013.

[38] E. Sloane, A. Ledeboer, W. Seibert, B. Coats, M. Van Strien, S. Maier, K. Johnson, R. Chavez, L. Watkins, L. Leinwand, Anti-inflammatory cytokine gene therapy decreases sensory and motor dysfunction in experimental Multiple Sclerosis: MOG-EAE behavioral and anatomical symptom treatment with cytokine gene therapy, Brain Behav. Immun. 23 (2009) 92–100, https://doi.org/10.1016/j.bbi.2008.09.004.

[39] N. Dos Santos, L.S. Novaes, G. Dragunas, J.R. Rodrigues, W. Brandão, R. Camarini, J.P.S. Peron, C.D. Munhoz, High dose of dexamethasone protects against EAE-induced motor deficits but impairs learning/memory in C57BL/6 mice, Sci. Rep. 9 (2019) 6673, https://doi.org/10.1038/s41598-019-43217-3.

[40] A. Lieu, G. Tenorio, B.J. Kerr, Protein kinase C gamma (PKCγ) as a novel marker to assess the functional status of the corticospinal tract in experimental autoimmune encephalomyelitis (EAE), J. Neuroimmunol. 256 (2013) 43–48, https://doi.org/10.1016/j.jneuroim.2013.01.003.

[41] R.E. Klaren, R.W. Motl, J.A. Woods, S.D. Miller, Effects of exercise in experimental autoimmune encephalomyelitis (an animal model of multiple sclerosis), J. Neuroimmunol. 274 (2014) 14–19, https://doi.org/10.1016/j.jneuroim.2014.06.014.

[42] A.P. Robinson, C.T. Harp, A. Noronha, S.D. Miller, The experimental autoimmune encephalomyelitis (EAE) model of MS: utility for understanding disease pathophysiology and treatment, Handb. Clin. Neurol. 122 (2014) 173–189, https://doi.org/10.1016/B978-0-444-52001-2.00008-X.

[43] F.G. Goh, K.S. Midwood, Intrinsic danger: activation of Toll-like receptors in rheumatoid arthritis, Rheumatology 51 (2012) 7–23, https://doi.org/10.1093/rheumatology/ker257.

[44] M.A. Saad, A.E. El-Sahhar, H.H. Arab, M.Y. Al-Shorbagy, Nicorandil abates arthritic perturbations induced by complete Freund's adjuvant in rats via conquering TLR4-MyD88-TRAF6 signaling pathway, Life Sci. 218 (2019) 284–291, https://doi.org/10.1016/j.lfs.2019.01.002.

[45] M. Farrugia, B. Baron, The role of toll-like receptors in autoimmune diseases through failure of the self-recognition mechanism, Int J Inflam. 2017 (2017), https://doi.org/10.1155/2017/8391230.

[46] C. Zheng, J. Chen, F. Chu, J. Zhu, T. Jin, Inflammatory role of TLR-MyD88 signaling in multiple sclerosis, Front. Mol. Neurosci. 12 (2019), https://doi.org/10.3389/fnmol.2019.00314.

[47] A.J. Kwilasz, S.M.G. Fulgham, J.C. Duran-Malle, A.E. Schrama, E.H. Mitten, L. S. Todd, H.P. Patel, T.A. Larson, M.A. Clements, K.M. Harris, Toll-like receptor 2 and 4 antagonism for the treatment of experimental autoimmune encephalomyelitis (EAE)-related pain, Brain Behav. Immun. 93 (2021) 80–95, https://doi.org/10.1016/j.bbi.2020.12.016.

[48] W. Xiang, Z.-Y. Chao, D.-Y. Feng, Role of Toll-like receptor/MYD88 signaling in neurodegenerative diseases, Rev. Neurosci. 26 (2015) 407–414, https://doi.org/10.1515/revneuro-2014-0067.

[49] S. Akira, K. Takeda, Toll-like receptor signalling, Nat. Rev. Immunol. 4 (2004) 499–511, https://doi.org/10.1038/nri1391.

[50] D. Martorelli, E. Muraro, A. Merlo, R. Turrini, A. Rosato, R. Dolcetti, Role of CD4+ cytotoxic T lymphocytes in the control of viral diseases and cancer, Int. Rev. Immunol. 29 (2010) 371–402, https://doi.org/10.3109/08830185.2010.489658.

[51] Y. Zhao, Z. Yang, Y. He, R. Sun, H. Yuan, The KATP channel opener, nicorandil, ameliorates brain damage by modulating synaptogenesis after ischemic stroke, PLoS One 16 (2021) e0246019.

[52] U. Okkay, I.F. Okkay, Neuroprotective effect of nicorandil in 6-OHDA induced in vitro model of parkinson's disease, Med. Sci. 11 (2022) 224–227, https://doi.org/10.5455/medscience.2021.07.231.

[53] W.U. Koh, J. Kim, J. Lee, G.-W. Song, G.S. Hwang, E. Tak, J.-G. Song, Remote ischemic preconditioning and diazoxide protect from hepatic ischemic reperfusion injury by inhibiting HMGB1-induced TLR4/MyD88/NF-κB signaling, Int. J. Mol. Sci. 20 (2019) 5899, https://doi.org/10.3390/ijms20235899.

[54] P. Pifarre, J. Prado, M.A. Baltrons, M. Giralt, P. Gabarro, D.L. Feinstein, J. Hidalgo, A. Garcia, Sildenafil (Viagra) ameliorates clinical symptoms and neuropathology in a mouse model of multiple sclerosis, Acta Neuropathol. 121 (2011) 499–508, https://doi.org/10.1007/s00401-010-0795-6.

[55] T.A. Yahaya, S.O. Adeola, U.U. Emma, Neuro-protective effect of Carvedilol, an adrenergic antagonist against scopolamine-induced cognitive impairment in mice, J. Appl. Pharm. Sci. 3 (2013) S32–S36, https://doi.org/10.7324/JAPS.2013.38.S6.

[56] K. Oettl, J. Greilberger, K. Zangger, E. Haslinger, G. Reibnegger, G. Jürgens, Radical-scavenging and iron-chelating properties of carvedilol, an antihypertensive drug with antioxidative activity, Biochem. Pharmacol. 62 (2001) 241–248, https://doi.org/10.1016/s0006-2952(01)00651-7.

[57] P. Kumar, A. Kumar, Prolonged pretreatment with carvedilol prevents 3-nitropropionic acid-induced behavioral alterations and oxidative stress in rats, Pharmacol. Rep. 60 (2008) 706.

[58] Y. Gilgun-Sherki, E. Melamed, D. Offen, The role of oxidative stress in the pathogenesis of multiple sclerosis: the need for effective antioxidant therapy, J. Neurol. 251 (2004) 261–268, https://doi.org/10.1007/s00415-004-0348-9.

[59] R. Chen, R. Kang, D. Tang, The mechanism of HMGB1 secretion and release, Exp. Mol. Med. 54 (2022) 91–102, https://doi.org/10.1038/s12276-022-00736-w.

[60] T. Liu, L. Zhang, D. Joo, S.-C. Sun, NF-κB signaling in inflammation, Signal Transduct. Target. Ther. 2 (2017) 1–9, https://doi.org/10.1038/sigtrans.2017.23.

[61] H. Villarroya, Y. Marie, J.C. Ouallet, F.L. Saux, J.L. Tchélingérian, N. Baumann, Expression of TNFα in central neurons of Lewis rat spinal cord after EAE induction, J. Neurosci. Res. 49 (1997) 592–599, https://doi.org/10.1002/(SICI)1097-4547(19970901)49:5<592::AID-JNR9>3.0.CO;2-6.

[62] A. Jebali, M.N. Karimabad, Z. Ahmadi, H. Khorramdel, A. Kaeidi, M. Mirzaei, M. Zare-Bidaki, H. Ahmadinia, A. Vakilian, A. Darekordi, Attenuation of inflammatory response in the EAE model by PEGlated nanoliposome of pistachio

oils, J. Neuroimmunol. 347 (2020) 577352, https://doi.org/10.1016/j.jneuroim.2020.577352.
[63] Q. Yang, C. Zheng, J. Cao, G. Cao, P. Shou, L. Lin, T. Velletri, M. Jiang, Q. Chen, Y. Han, Spermidine alleviates experimental autoimmune encephalomyelitis through inducing inhibitory macrophages, Cell Death Differ. 23 (2016) 1850–1861, https://doi.org/10.1038/cdd.2016.71.
[64] Y.-J. Zhang, A.-Q. Zhang, X.-X. Zhao, Z.-L. Tian, L. Yao, Nicorandil protects against ischaemia-reperfusion injury in newborn rat kidney, Pharmacology 92 (2013) 245–256, https://doi.org/10.1159/000355060.
[65] H. Liu, W. Li, W. Gu, Y. Kong, N. Yang, L. Chen, Immunoregulatory effects of carvedilol on rat experimental autoimmune myocarditis, Scand. J. Immunol. 71 (2010) 38–44, https://doi.org/10.1111/j.1365-3083.2009.02347.x.
[66] E.S. Wohleb, M.L. Hanke, A.W. Corona, N.D. Powell, M.S. La'Tonia, M.T. Bailey, R. J. Nelson, J.P. Godbout, J.F. Sheridan, β-Adrenergic receptor antagonism prevents anxiety-like behavior and microglial reactivity induced by repeated social defeat, J. Neurosci. 31 (2011) 6277–6288, https://doi.org/10.1523/JNEUROSCI.0450-11.2011.
[67] S. Éliás, A. Schmidt, V. Kannan, J. Andersson, J. Tegnér, TGF-β affects the differentiation of human GM-CSF+ CD4+ T cells in an activation-and sodium-dependent manner, Front. Immunol. 7 (2016) 603, https://doi.org/10.3389/fimmu.2016.00603.
[68] L.M. Peeters, M. Vanheusden, V. Somers, B. Van Wijmeersch, P. Stinissen, B. Broux, N. Hellings, Cytotoxic CD4+ T cells drive multiple sclerosis progression, Front. Immunol. 8 (2017) 1160, https://doi.org/10.3389/fimmu.2017.01160.
[69] M. Rafei, P.M. Campeau, A. Aguilar-Mahecha, M. Buchanan, P. Williams, E. Birman, S. Yuan, Y.K. Young, M.-N. Boivin, K. Forner, Mesenchymal stromal cells ameliorate experimental autoimmune encephalomyelitis by inhibiting CD4 Th17 T cells in a CC chemokine ligand 2-dependent manner, J. Immunol. 182 (2009) 5994–6002, https://doi.org/10.4049/jimmunol.0803962.
[70] M.O. Li, Y.Y. Wan, S. Sanjabi, A.-K.-L. Robertson, R.A. Flavell, Transforming growth factor-β regulation of immune responses, Annu. Rev. Immunol. 24 (2006) 99–146, https://doi.org/10.1146/annurev.immunol.24.021605.090737.
[71] J. Luo, P.P. Ho, M.S. Buckwalter, T. Hsu, L.Y. Lee, H. Zhang, D.-K. Kim, S.-J. Kim, S. S. Gambhir, L. Steinman, Glia-dependent TGF-β signaling, acting independently of the TH17 pathway, is critical for initiation of murine autoimmune encephalomyelitis, The, J. Clin. Invest. 117 (2007) 3306–3315, https://doi.org/10.1172/JCI31763.
[72] P.R. Mangan, L.E. Harrington, D.B. O'Quinn, W.S. Helms, D.C. Bullard, C.O. Elson, R.D. Hatton, S.M. Wahl, T.R. Schoeb, C.T. Weaver, Transforming growth factor-β induces development of the TH17 lineage, Nature 441 (2006) 231–234, https://doi.org/10.1038/nature04754. Epub 2006 Apr 30.
[73] D.J. Cua, J. Sherlock, Y. Chen, C.A. Murphy, B. Joyce, B. Seymour, L. Lucian, W. To, S. Kwan, T. Churakova, Interleukin-23 rather than interleukin-12 is the critical cytokine for autoimmune inflammation of the brain, Nature 421 (2003) 744–748, https://doi.org/10.1038/nature01355.
[74] C.L. Langrish, Y. Chen, W.M. Blumenschein, J. Mattson, B. Basham, J.D. Sedgwick, T. McClanahan, R.A. Kastelein, D.J. Cua, IL-23 drives a pathogenic T cell population that induces autoimmune inflammation, J. Exp. Med. 201 (2005) 233–240, https://doi.org/10.1084/jem.20041257.
[75] J.S. Tzartos, M.A. Friese, M.J. Craner, J. Palace, J. Newcombe, M.M. Esiri, L. Fugger, Interleukin-17 production in central nervous system-infiltrating T cells and glial cells is associated with active disease in multiple sclerosis, Am. J. Pathol. 172 (2008) 146–155, https://doi.org/10.2353/ajpath.2008.070690.
[76] N. Grigoriadis, V. Van Pesch, A basic overview of multiple sclerosis immunopathology, Eur. J. Neurol. 22 (2015) 3–13, https://doi.org/10.1111/ene.12798.
[77] R. Dringen, Oxidative and antioxidative potential of brain microglial cells, Antioxi. Redox Signal. 7 (2005) 1223–1233, https://doi.org/10.1089/ars.2005.7.1223.
[78] I. Tasset, E. Agüera, F. Sánchez-López, M. Feijóo, A.I. Giraldo, A.H. Cruz, F. Gascón, I. Túnez, Peripheral oxidative stress in relapsing–remitting multiple sclerosis, Clin. Biochem. 45 (2012) 440–444, https://doi.org/10.1016/j.clinbiochem.2012.01.023.
[79] J. Witherick, A. Wilkins, N. Scolding, K. Kemp, Mechanisms of oxidative damage in multiple sclerosis and a cell therapy approach to treatment, Autoimmune Dis. 2011 (2010), https://doi.org/10.4061/2011/164608.
[80] L. Haider, M.T. Fischer, J.M. Frischer, J. Bauer, R. Höftberger, G. Botond, H. Esterbauer, C.J. Binder, J.L. Witztum, H. Lassmann, Oxidative damage in multiple sclerosis lesions, Brain 134 (2011) 1914–1924, https://doi.org/10.1093/brain/awr128.
[81] Y. He, M. Du, Y. Gao, H. Liu, H. Wang, X. Wu, Z. Wang, Astragaloside IV attenuates experimental autoimmune encephalomyelitis of mice by counteracting oxidative stress at multiple levels, PLoS One 8 (2013) e76495.
[82] W. Xu, T. Zhao, H. Xiao, The implication of oxidative stress and AMPK-Nrf2 antioxidative signaling in pneumonia pathogenesis, Front. Endocrinol. 11 (2020) 400, https://doi.org/10.3389/fendo.2020.00400.
[83] R. Ibitoye, K. Kemp, C. Rice, K. Hares, N. Scolding, A. Wilkins, Oxidative stress-related biomarkers in multiple sclerosis: a review, Biomark Med. 10 (2016) 889–902, https://doi.org/10.2217/bmm-2016-0097.
[84] S. Ljubisavljevic, I. Stojanovic, D. Pavlovic, D. Sokolovic, I. Stevanovic, Aminoguanidine and N-acetyl-cysteine supress oxidative and nitrosative stress in EAE rat brains, Redox Rep. 16 (2011) 166–172, https://doi.org/10.1179/1351000211Y.0000000007.
[85] H. Chen, Y. Fang, W. Li, R.C. Orlando, N. Shaheen, X.L. Chen, NFkB and Nrf2 in esophageal epithelial barrier function, Tissue Barriers 1 (2013) e27463.
[86] Y. Zhang, X. Yang, X. Ge, F. Zhang, Puerarin attenuates neurological deficits via Bcl-2/Bax/cleaved caspase-3 and Sirt3/SOD2 apoptotic pathways in subarachnoid hemorrhage mice, Biomed. Pharmacother. 109 (2019) 726–733, https://doi.org/10.1016/j.biopha.2018.10.161.
[87] A. Kumari, P. Kakkar, Lupeol prevents acetaminophen-induced in vivo hepatotoxicity by altering the Bax/Bcl-2 and oxidative stress-mediated mitochondrial signaling cascade, Life Sci. 90 (2012) 561–570, https://doi.org/10.1016/j.lfs.2012.01.012.
[88] X. Feng, H. Hou, Y. Zou, L. Guo, Defective autophagy is associated with neuronal injury in a mouse model of multiple sclerosis, Bosn. J. Basic Med. Sci. 17 (2017) 95, https://doi.org/10.17305/bjbms.2017.1696.
[89] T. Wada, J.M. Penninger, Mitogen-activated protein kinases in apoptosis regulation, Oncogene 23 (2004) 2838–2849, https://doi.org/10.1038/sj.onc.1207556.
[90] H. Liu, S. Liu, X. Tian, Q. Wang, J. Rao, Y. Wang, F. Xiang, H. Zheng, L. Xu, Z. Dong, Bexarotene Attenuates Focal Cerebral Ischemia-Reperfusion Injury via the Suppression of JNK/Caspase-3 Signaling Pathway, Neurochem. Res. 44 (2019) 2809–2820, https://doi.org/10.1007/s11064-019-02902-5.
[91] M.A. Ahmed, A.A. Ahmed, E.M. El Morsy, Acetyl-11-keto-β-boswellic acid prevents testicular torsion/detorsion injury in rats by modulating 5-LOX/LTB4 and p38-MAPK/JNK/Bax/Caspase-3 pathways, Life Sci. 260 (2020), 118472, https://doi.org/10.1016/j.lfs.2020.118472.
[92] S. Nishikawa, T. Tatsumi, J. Shiraishi, S. Matsunaga, M. Takeda, A. Mano, M. Kobara, N. Keira, M. Okigaki, T. Takahashi, Nicorandil regulates Bcl-2 family proteins and protects cardiac myocytes against hypoxia-induced apoptosis, J. Mol. Cell. Cardiol. 40 (2006) 510–519, https://doi.org/10.1016/j.yjmcc.2006.01.020.
[93] A.G. Bakr, E.H. Hassanein, F.E. Ali, E.A. El-Shoura, Combined apocynin and carvedilol protect against cadmium-induced testicular damage via modulation of inflammatory response and redox-sensitive pathways, Life Sci. 311 (2022), 121152, https://doi.org/10.1016/j.lfs.2022.121152.